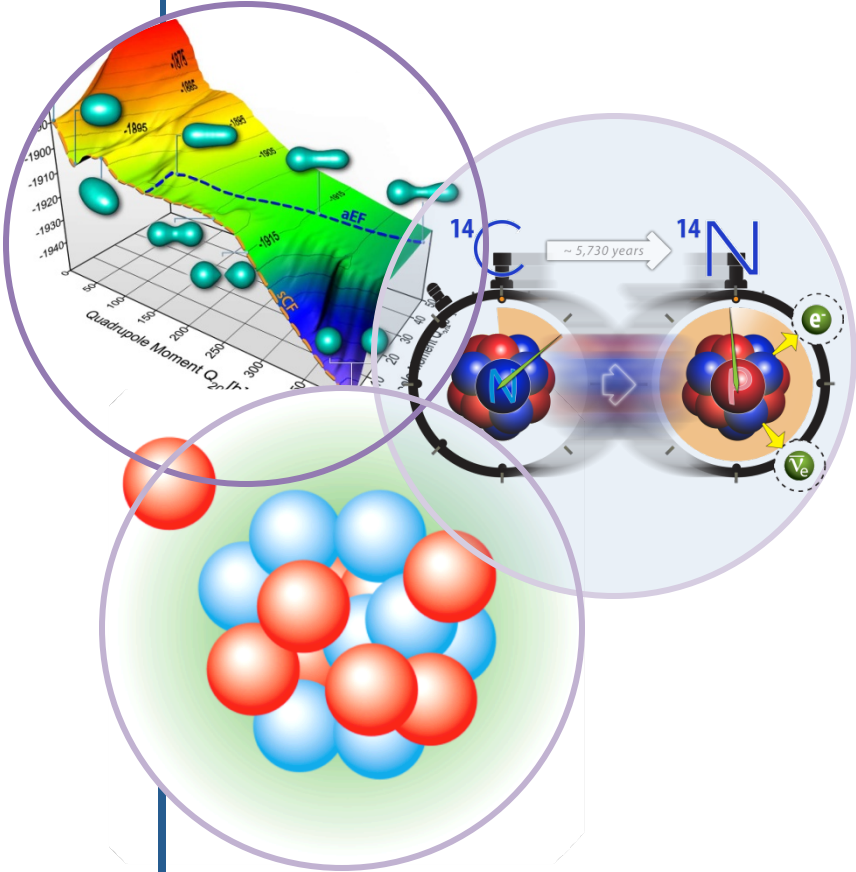


Coupled cluster approach to nuclear reactions and the role of continuum in neutron rich nuclei

Gaute Hagen (ORNL)



Lecture 5, TALENT school



Outline

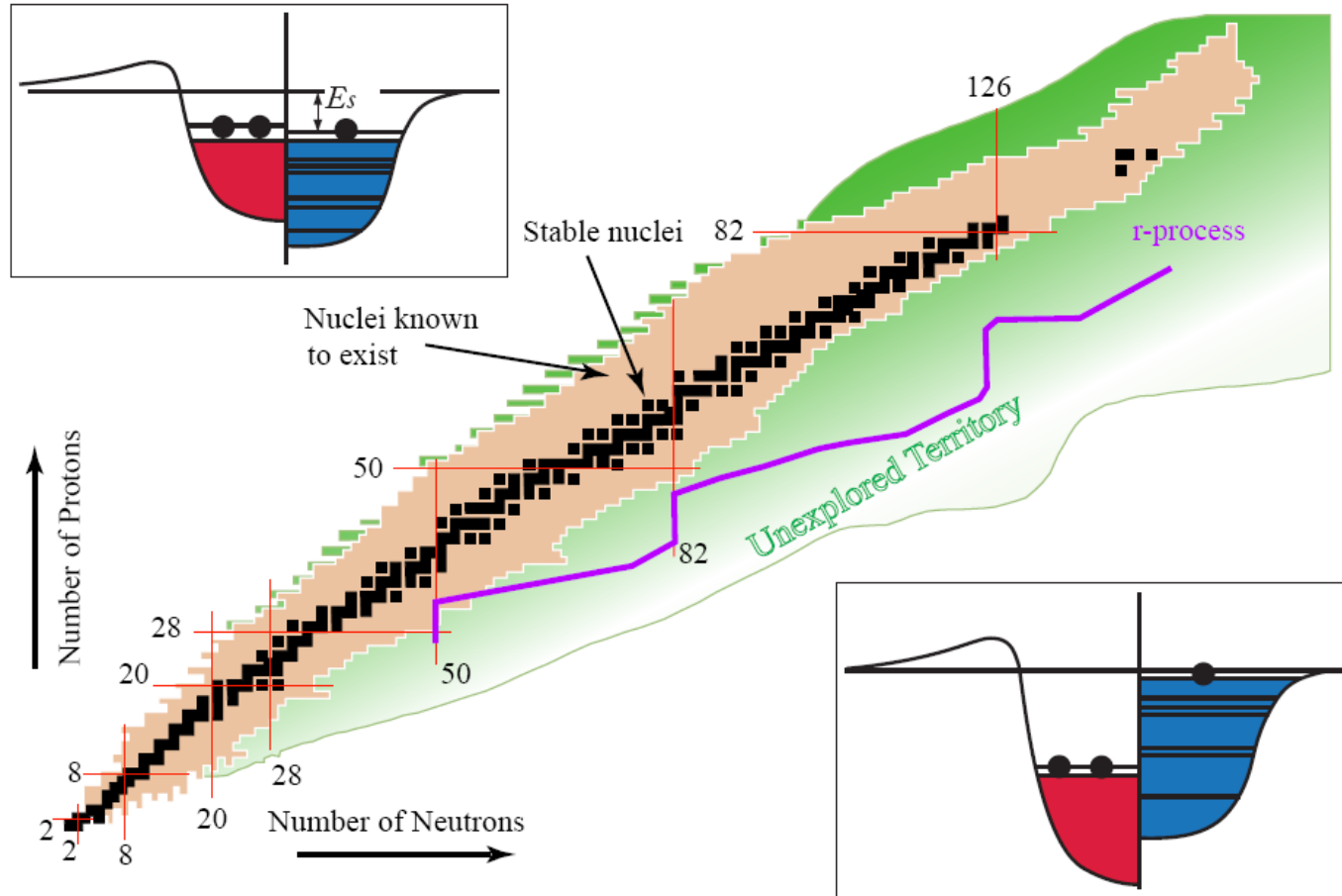
- The nucleus as an open quantum systems
 - Halos and Borromean nuclei
 - Treating resonances and bound-states on equal footing
- Role of continuum on level ordering in light nuclei
- Impact of continuum on the neutron dripline and the evolution of shell structure in calcium isotopes
- Extending CCM to study elastic scattering
 - Computing the overlap function from CCM
 - Spectroscopic factors and continuum induced correlations
 - Elastic proton scattering of ^{40}Ca and neutron scattering of ^{60}Ca
- Inelastic reactions and breakup observables from CCM
 - Computing the response function by combining the Lorentz Integral Transform technique with CCM
 - Dipole response from CCM in light and medium mass nuclei
 - Problem of saturation and impact on dipole response/
polarizability

Nuclear landscape and consequences.

~ 300 stable nuclei

$N/Z \sim 1$ for light nuclei

$N/Z \sim 1.5$ for ^{208}Pb



~4000-6000

unstable nuclei

decay by α , β , 1p,

2p,

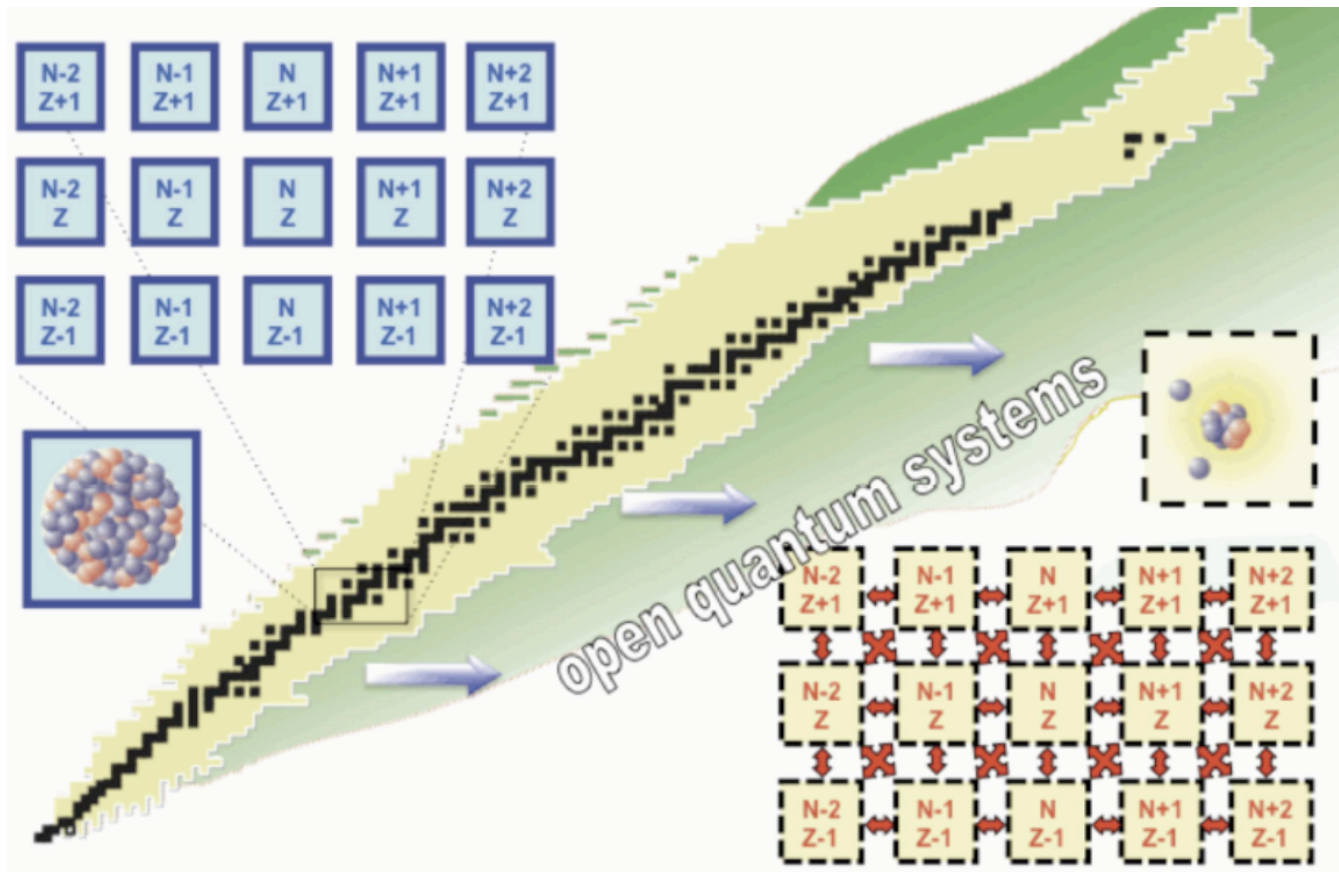
1n, cluster

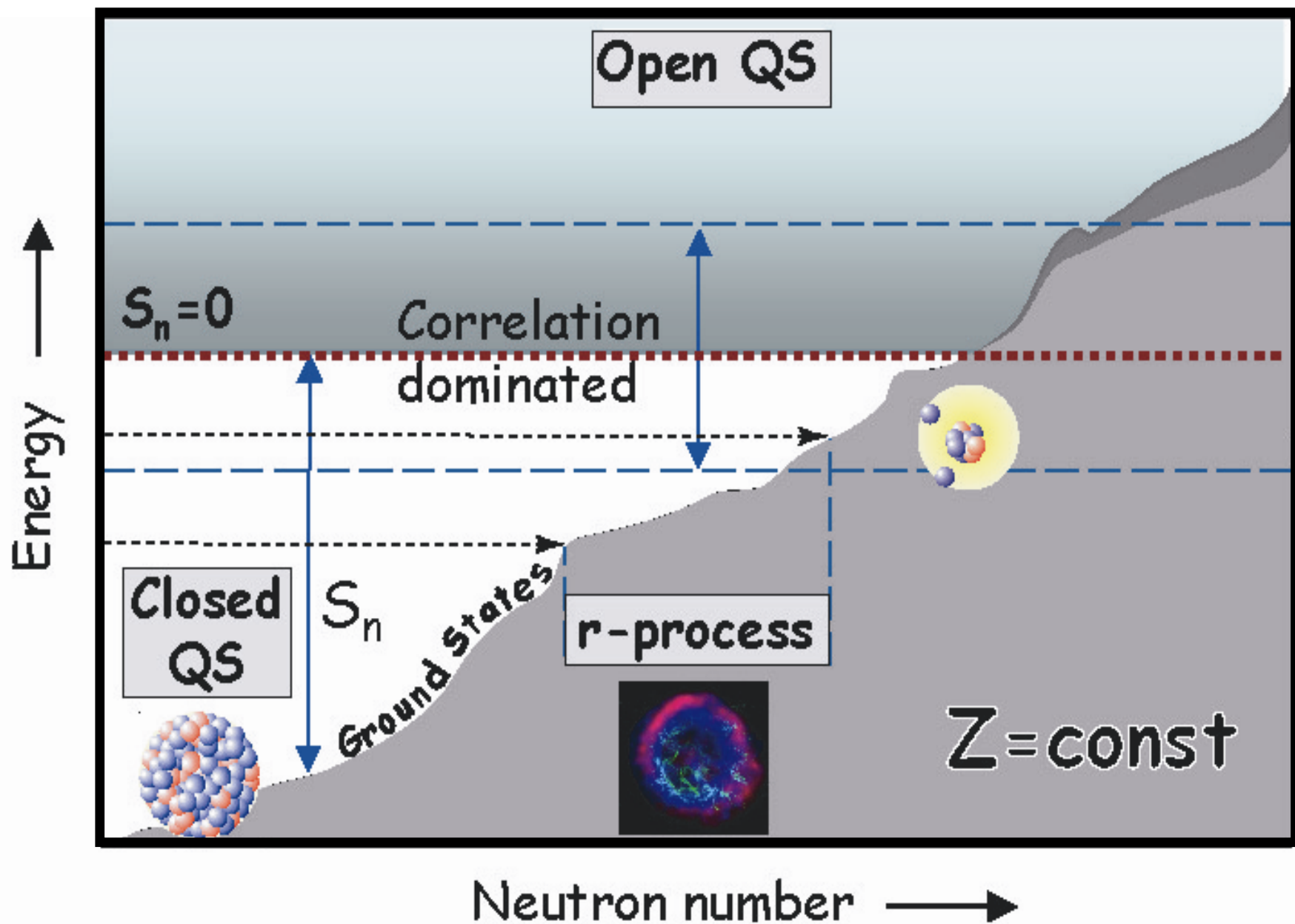
emission, fission...

Physics of nuclei at the edges of stability

From Wikipedia, the free encyclopedia:

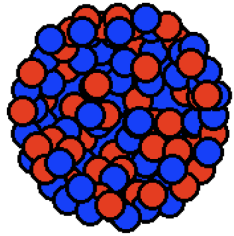
In physics, an open quantum system is a quantum system which is found to be in interaction with an external quantum system, the environment. The open quantum system can be viewed as a distinguished part of a larger closed quantum system, the other part being the environment.





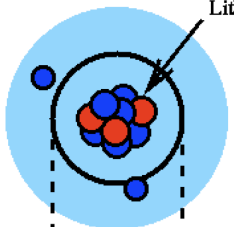
Nuclear halos a manifestation of openness

$$1 \text{ fm} = \frac{1}{10\,000\,000\,000\,000} \text{ cm}$$



Lead-208

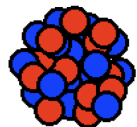
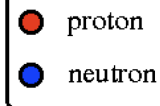
12 fm



Lithium-9

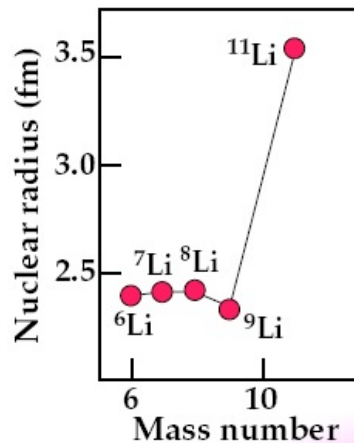
Lithium-11

7 fm



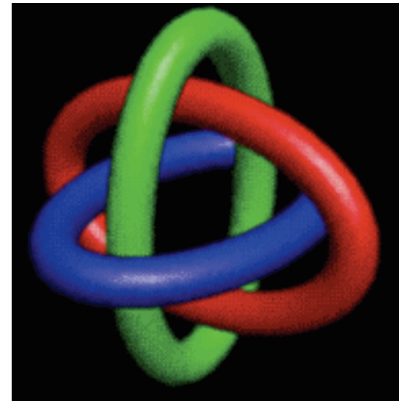
Calcium-48

- ^{11}Li matter radii unusually large compared to neighboring nuclei.
- ^{11}Li is the holy grail of nuclear halos I. Tanihata et al, Phys. Rev. Lett. **55**, 2676 (1985)



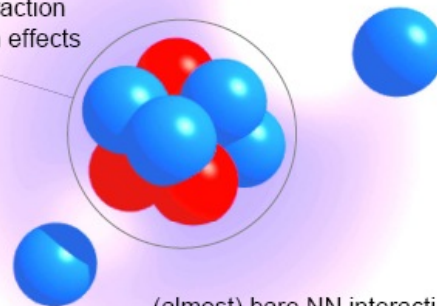
I. Tanihata et al.
Phys. Rev. Lett. 55, 2676 (1985)

Interaction cross section
measurements at Bevalac
(790 MeV/u)



Borromean rings

effective NN interaction
strong in-medium effects



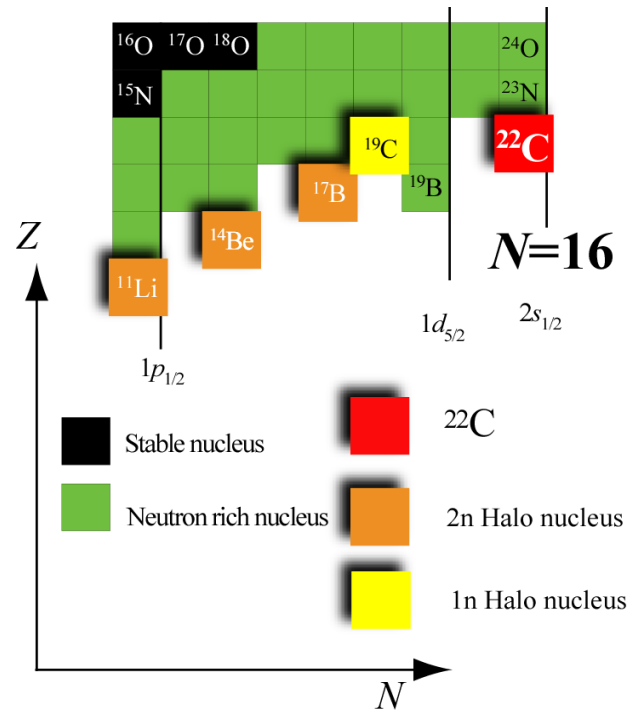
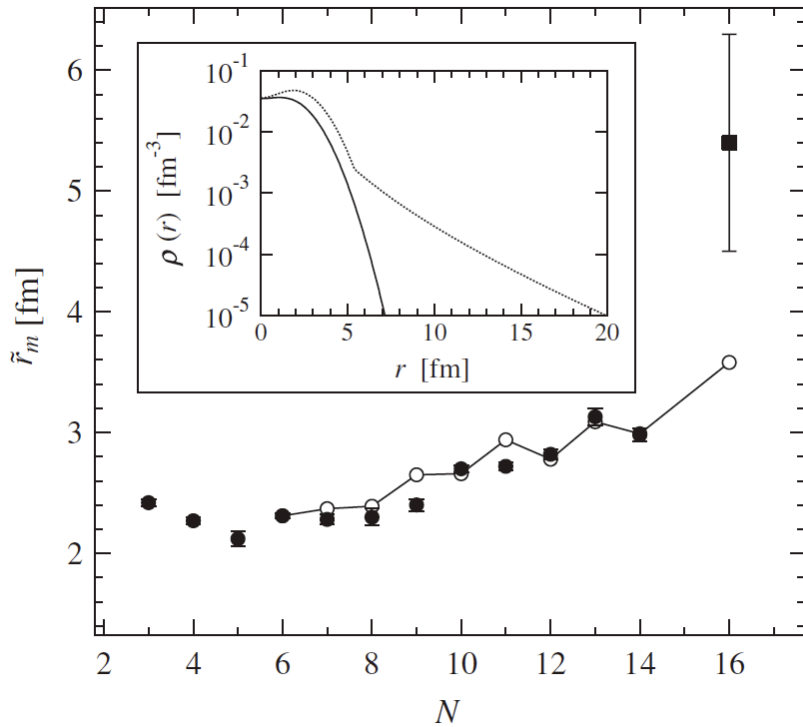
(almost) bare NN interaction
weak in-medium effects





Observation of a Large Reaction Cross Section in the Drip-Line Nucleus ^{22}C

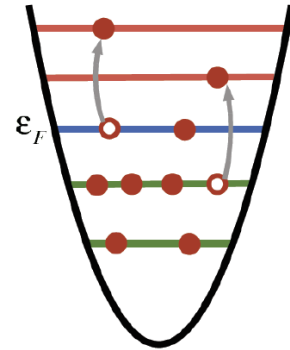
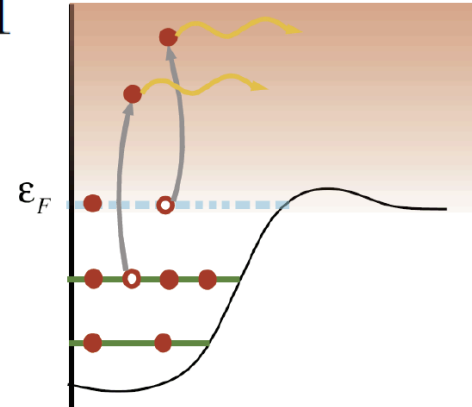
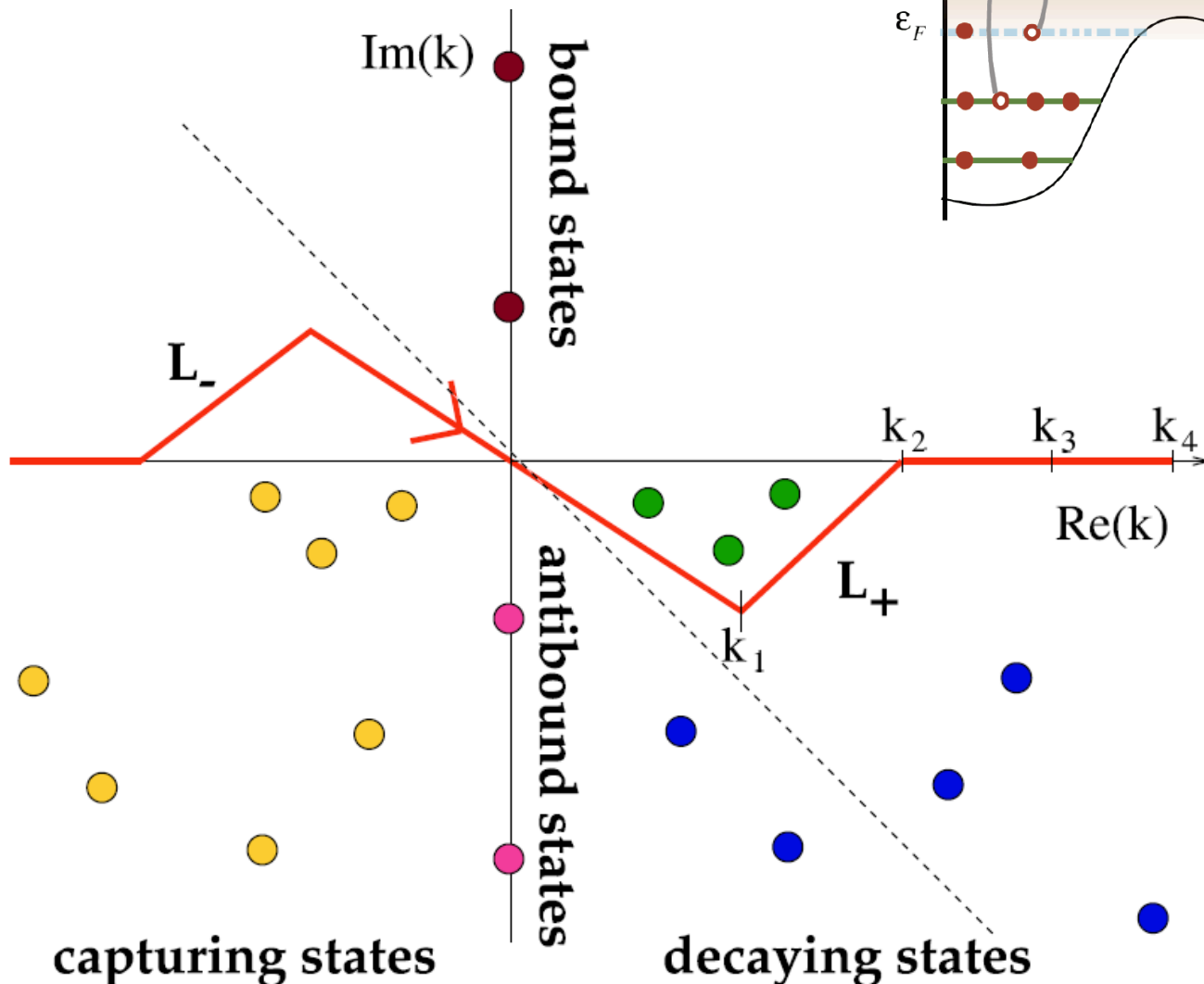
Carbon-22, which has a nucleus comprised of 16 neutrons and 6 protons, is the heaviest atom yet discovered to exhibit a "halo nucleus."



Physics of nuclei at the edges of stability

$$\sum_{n \in (b,d)} |u_n\rangle\langle u_n| + \int_{L^+} |u(k)\rangle\langle u(k)| dk = 1$$

T. Berggren Nucl. Phys. A 109 265 (1968)



The Berggren completeness treats bound, resonant and scattering states on equal footing.

Has been successfully applied in the shell model in the complex energy plane to light nuclei. For a review see

N. Michel et al J. Phys. G 36, 013101 (2009).

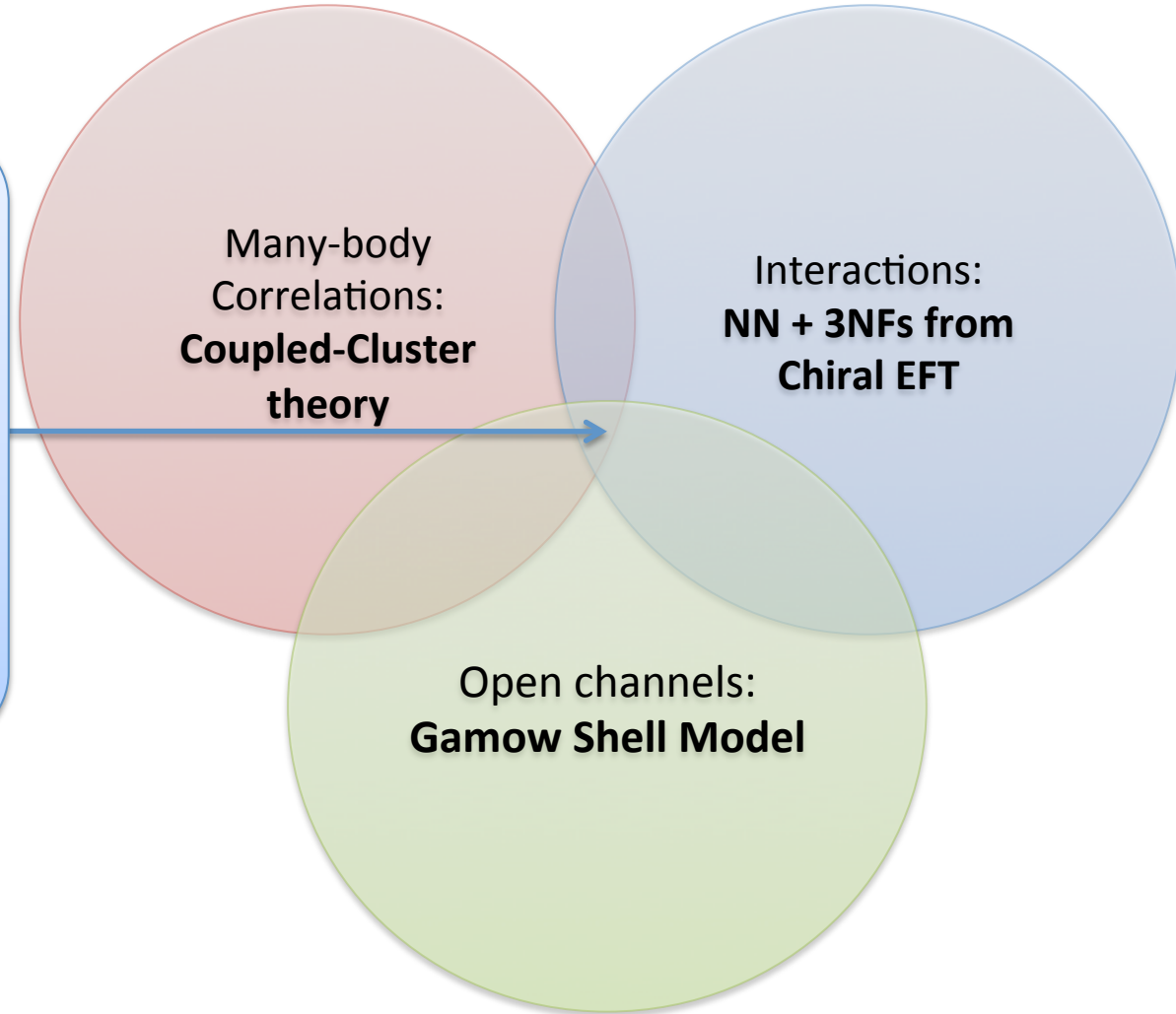
Physics of neutron rich nuclei is challenging and demanding

- Halo nuclei
- Neutron rich isotopes
- Clustering in nuclei, Hoyle state in ^{12}C
- New magic numbers appear at the driplines

Many-body
Correlations:
**Coupled-Cluster
theory**

Interactions:
**NN + 3NFs from
Chiral EFT**

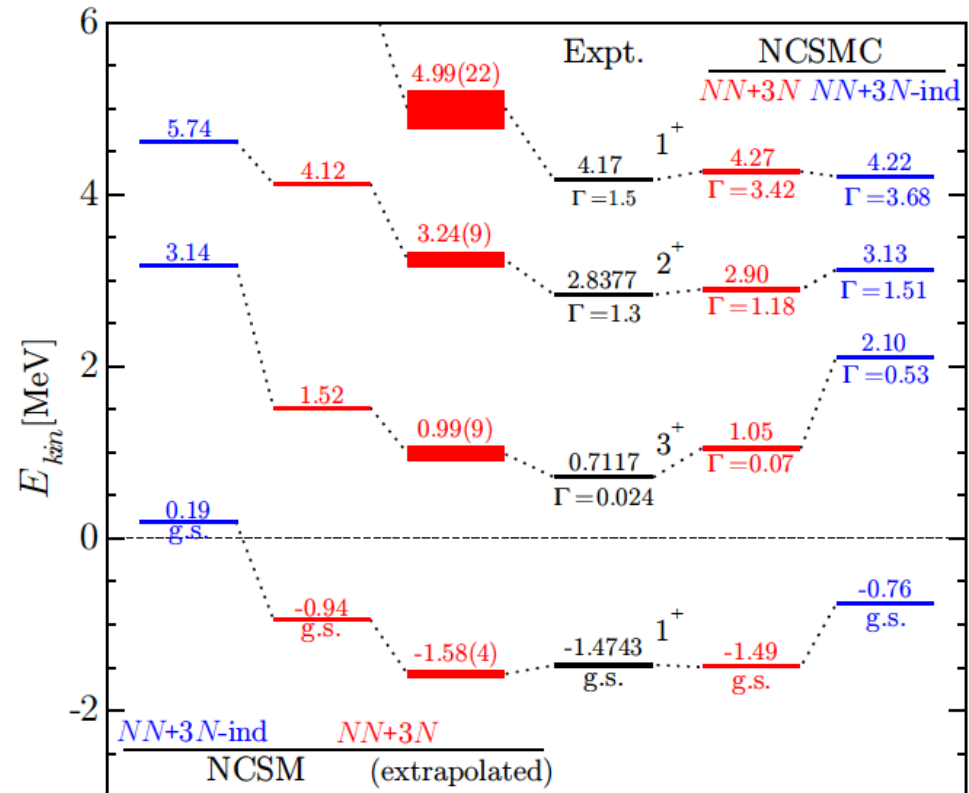
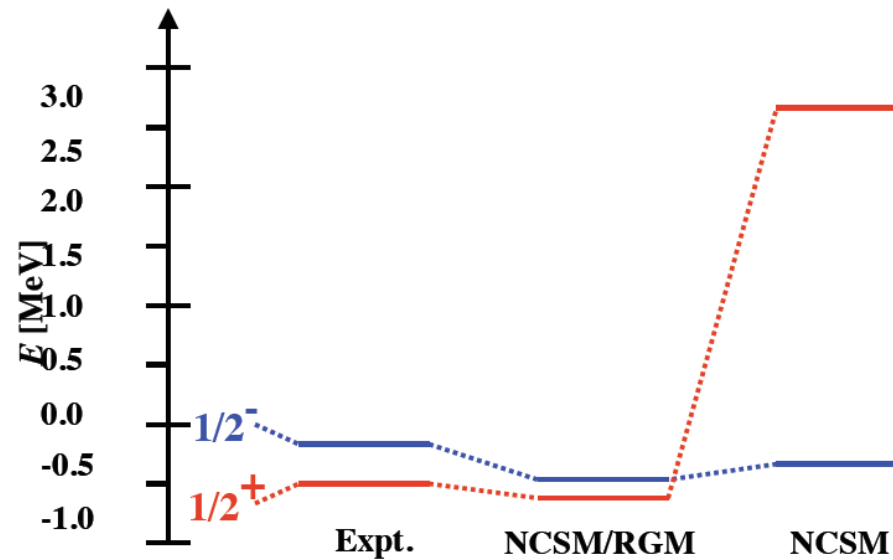
Open channels:
Gamow Shell Model



Ab-initio no-core shell model and resonating group method for scattering

First ab-initio description of the parity inverted ground state in ^{11}Be . S. Quaglioni and P. Navratil PRL (2008)

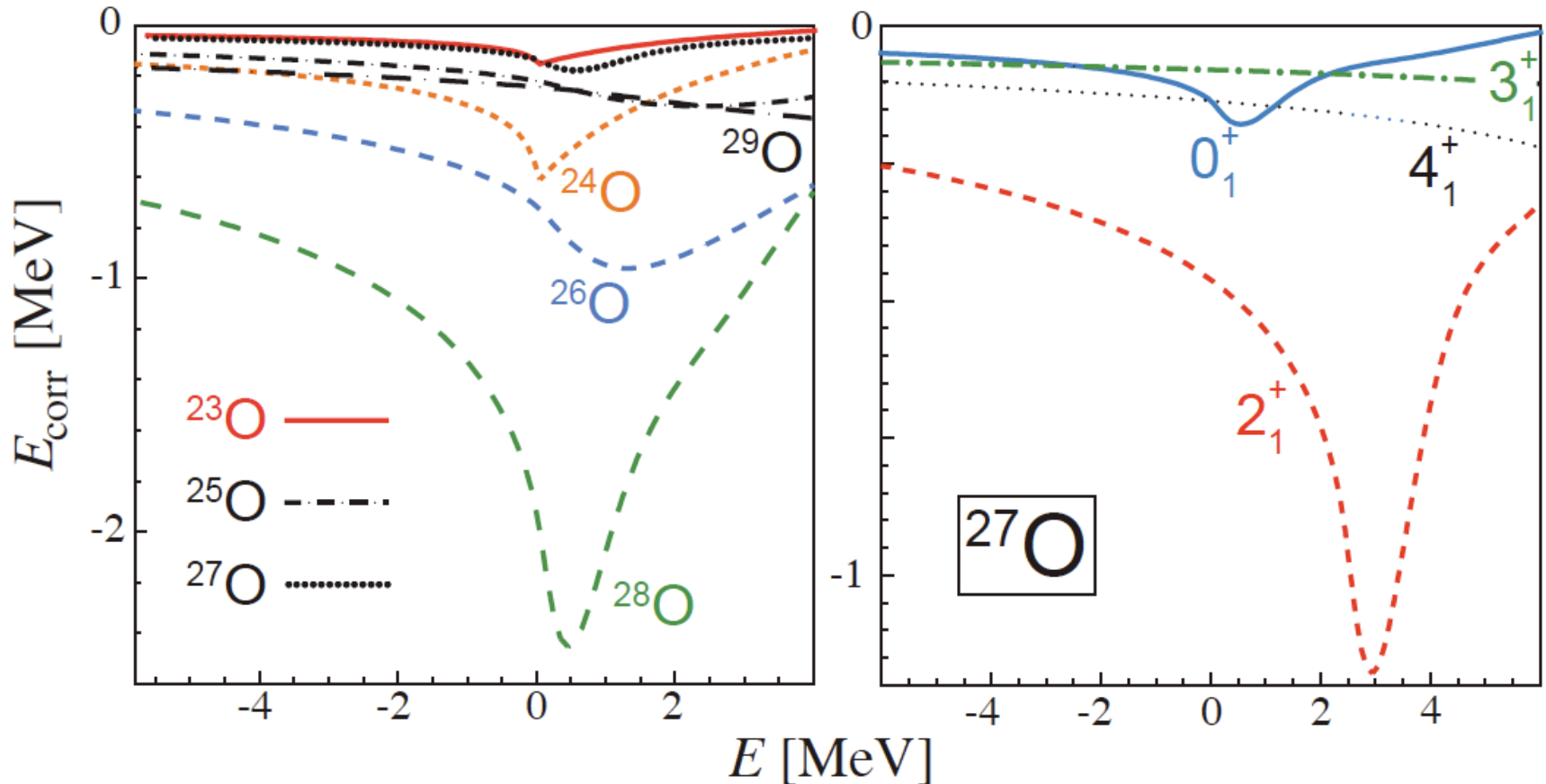
Spectra of ^6Li from NCSMC with chiral NN and 3NFs. Effect of continuum is significant on levels above the deuteron emission threshold. G. Hupin et al, PRL (2015)



Continuum induced correlations

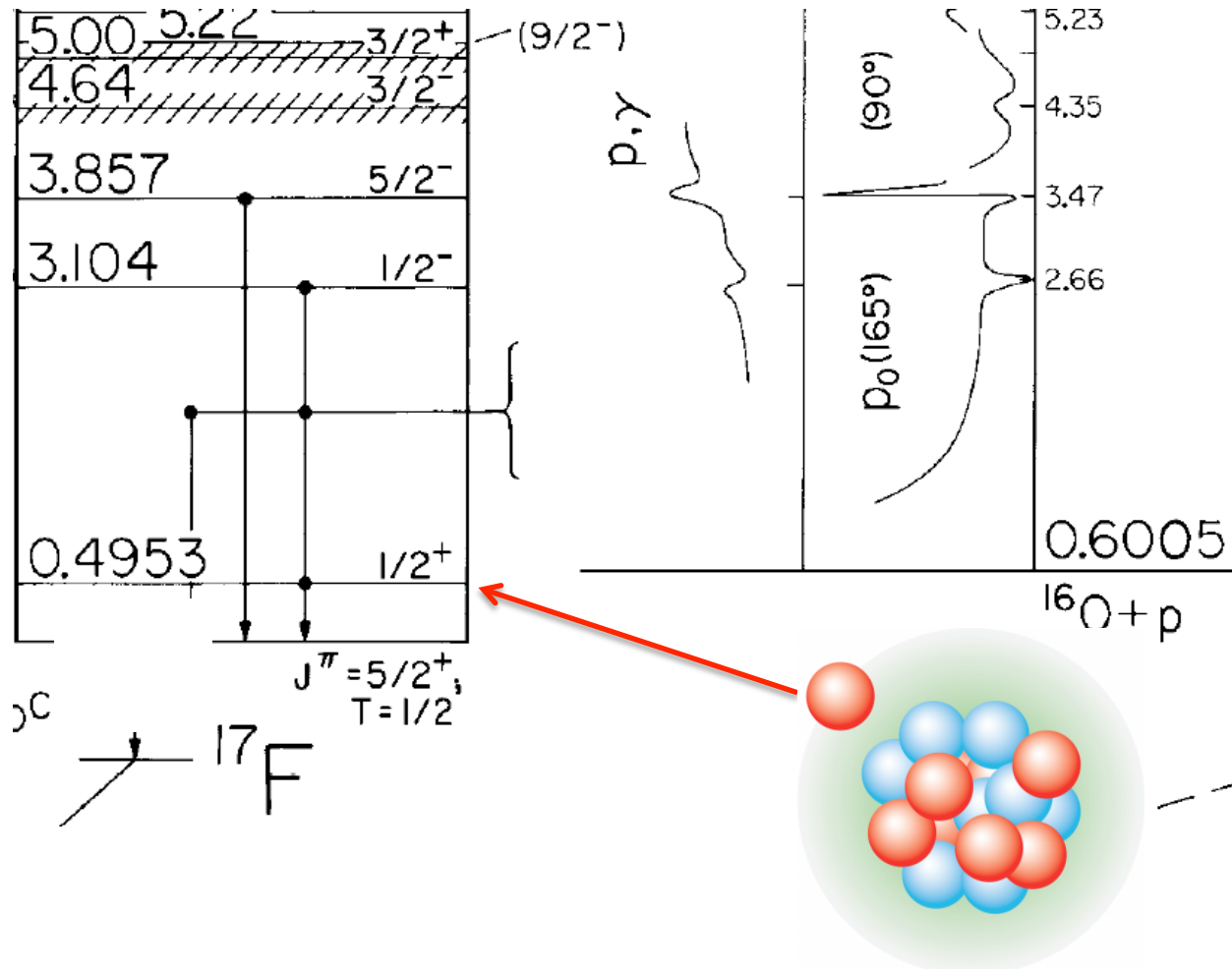
Continuum shell model calculations of oxygen isotopes. The effect of continuum correlations for nuclei with low neutron emission thresholds can be significant.

N. Michel et al, J. Phys. G **37** 064042 (2010).



Computing nuclei with A+1

Example: proton-halo state in ^{17}F



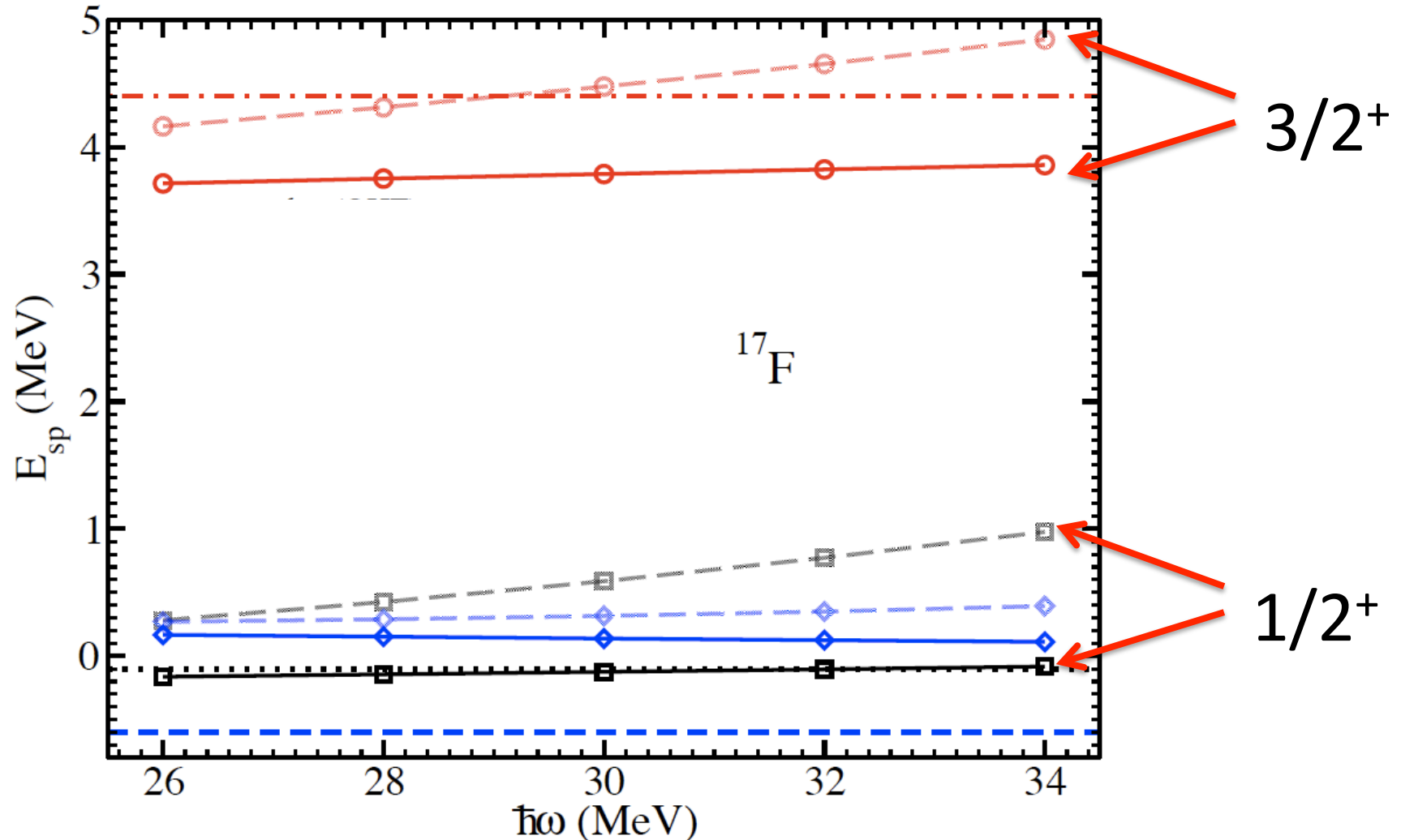
- Separation energy of halo state is only 105 keV
- Continuum has to be treated properly
- Use Berggren basis with PA-EOM-CCSD(2p1h)

Effect of continuum on low-lying states in ^{17}F

Single-particle basis consists of bound, resonance and scattering states

- Gamow basis for $s_{1/2}$, $d_{5/2}$ and $d_{3/2}$ single-particle states
- Harmonic oscillator states for other partial waves

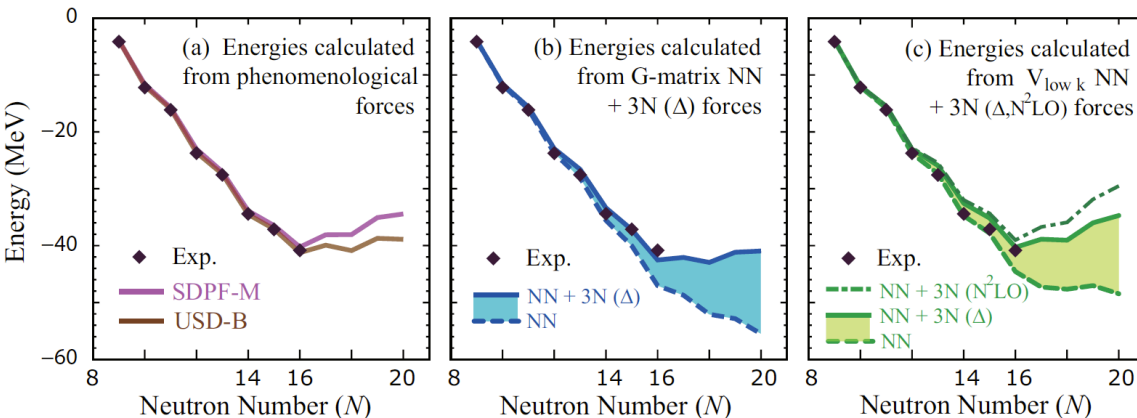
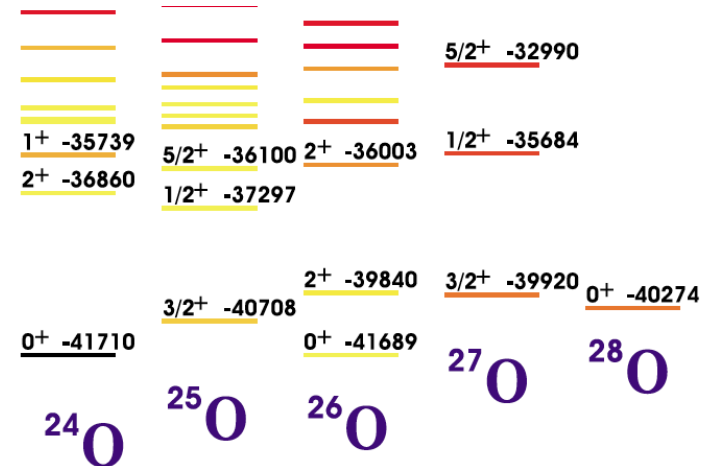
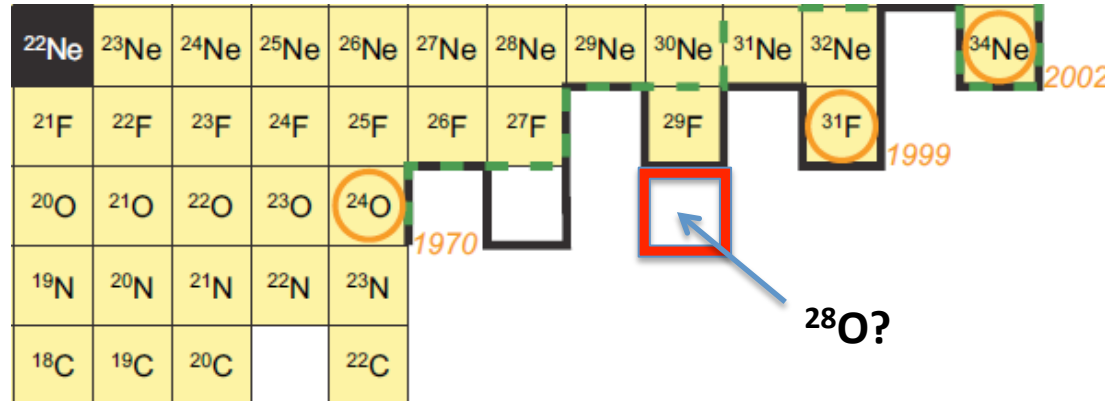
[G. Hagen, TP, M. Hjorth-Jensen,
Phys. Rev. Lett. 104, 182501 (2010)]



Is ^{28}O a bound nucleus?

Experimental situation

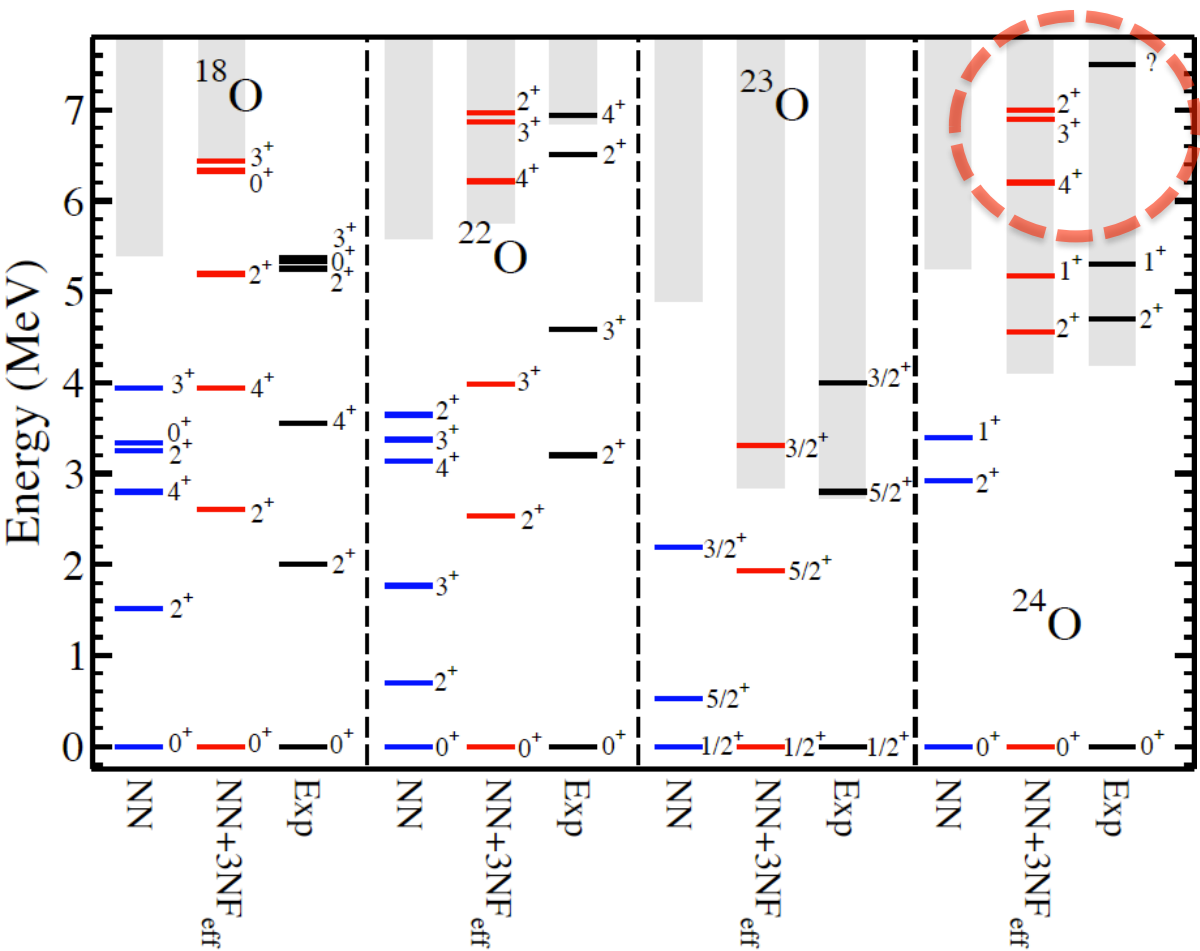
- “Last” stable oxygen isotope ^{24}O
- $^{25,26}\text{O}$ unstable (Hoffman et al 2008, Lunderberg et al 2012)
- ^{28}O not seen in experiments
- ^{31}F exists (adding on proton shifts drip line by 6 neutrons!?)



Continuum shell model with HBUSD interaction predict ^{28}O unbound. A. Volya and V. Zelevinsky PRL (2005)

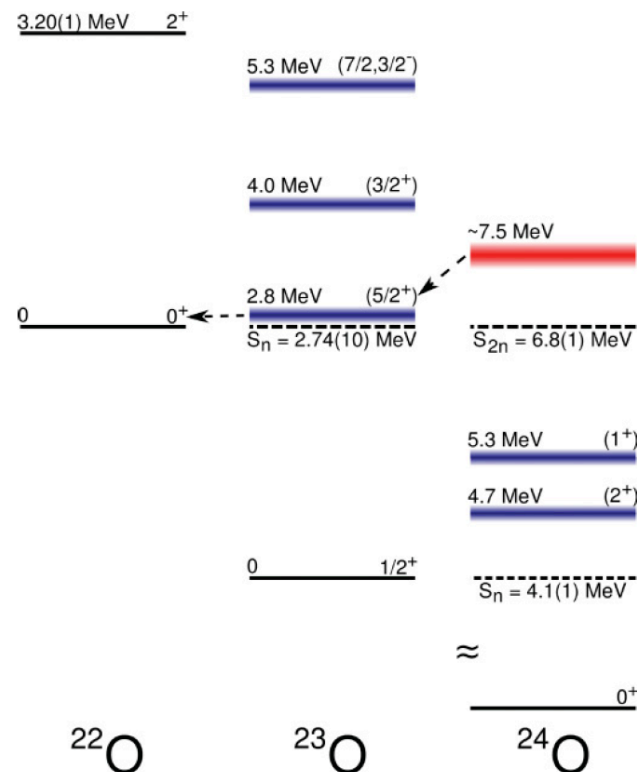
Shell model (sd shell) with monopole corrections based on three-nucleon force predicts ^{25}O as last stable isotope of oxygen. [Otsuka, Suzuki, Holt, Schwenk, Akaishi, PRL (2010), arXiv:0908.2607]

Excited states in neutron rich oxygen isotopes



Inclusion continuum and of schematic 3NFs:
 $k_F=1.05 \text{ fm}^{-1}$, $c_E=0.71$, $c_D=-0.2$

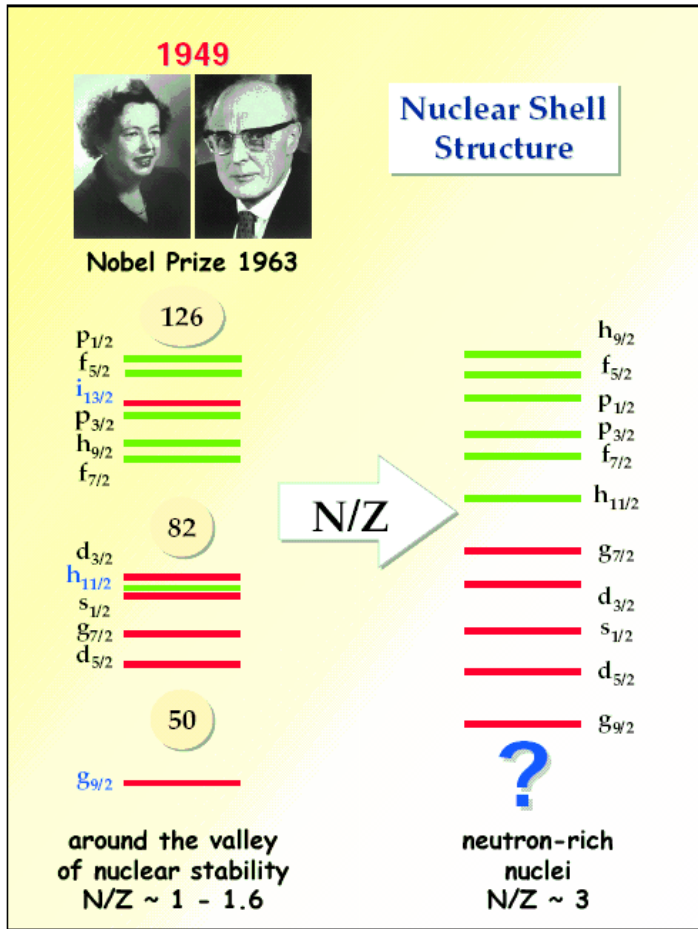
Hagen, Hjorth-Jensen, Jansen, Machleidt, Papenbrock,
 Phys. Rev. Lett. 108 242501 (2012)



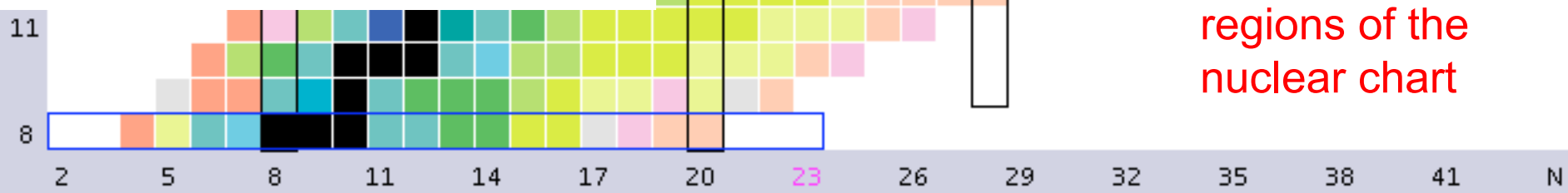
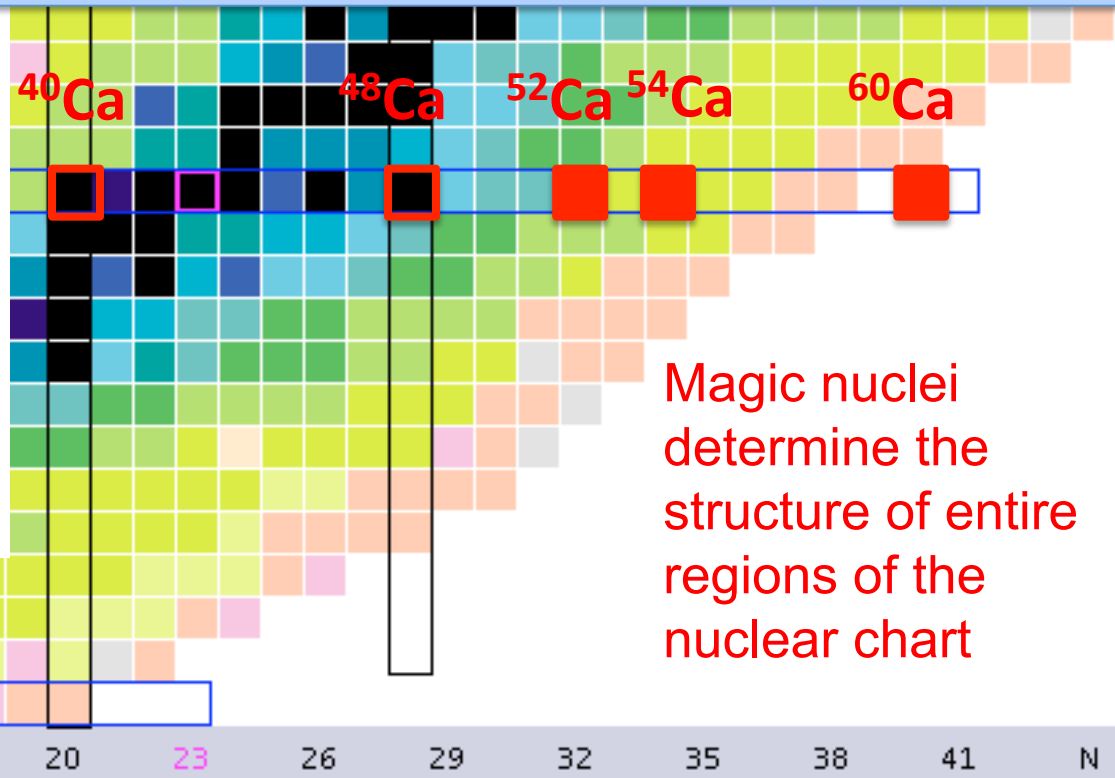
Experiment

[Hoffman et al., PRC 83, 031303 (2011)] Unbound states in ^{24}O populated by knockout from ^{26}F . Observation of ^{22}O and two-neutron cascade. Speculation: single resonance or superposition of states with $J^\pi=1^+$ to 4^+ .

Effect of continuum on shell structure in neutron rich Calcium



- How do shell closures and magic numbers evolve towards the dripline?
- Is the naïve shell model picture valid at the neutron dripline?
- What are the mechanisms for new shell structure?

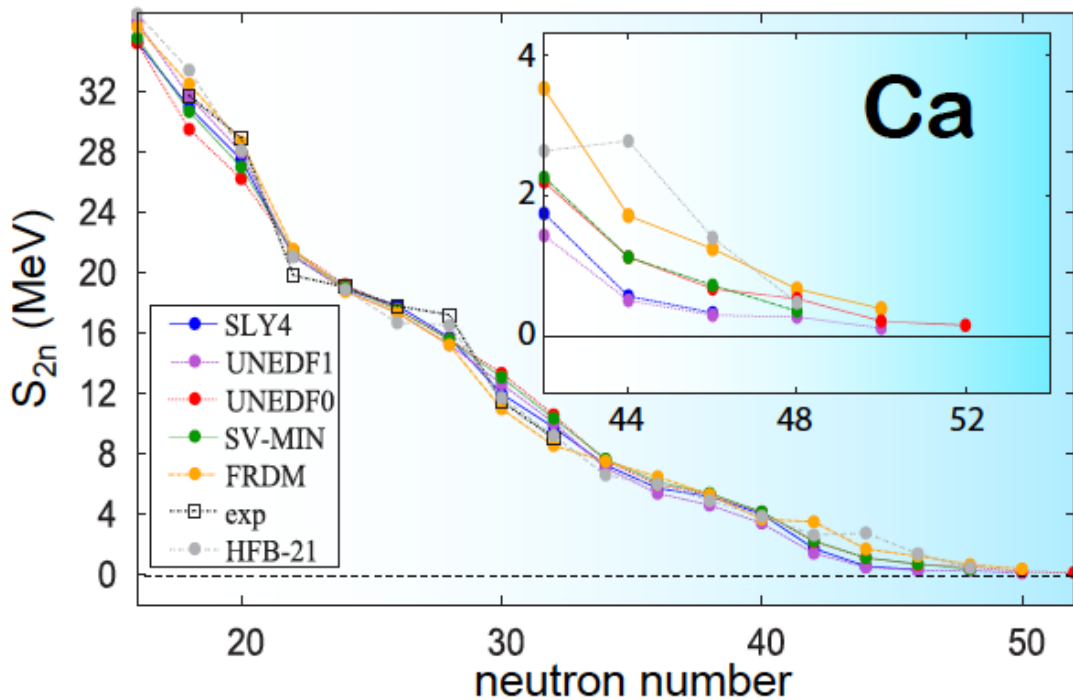
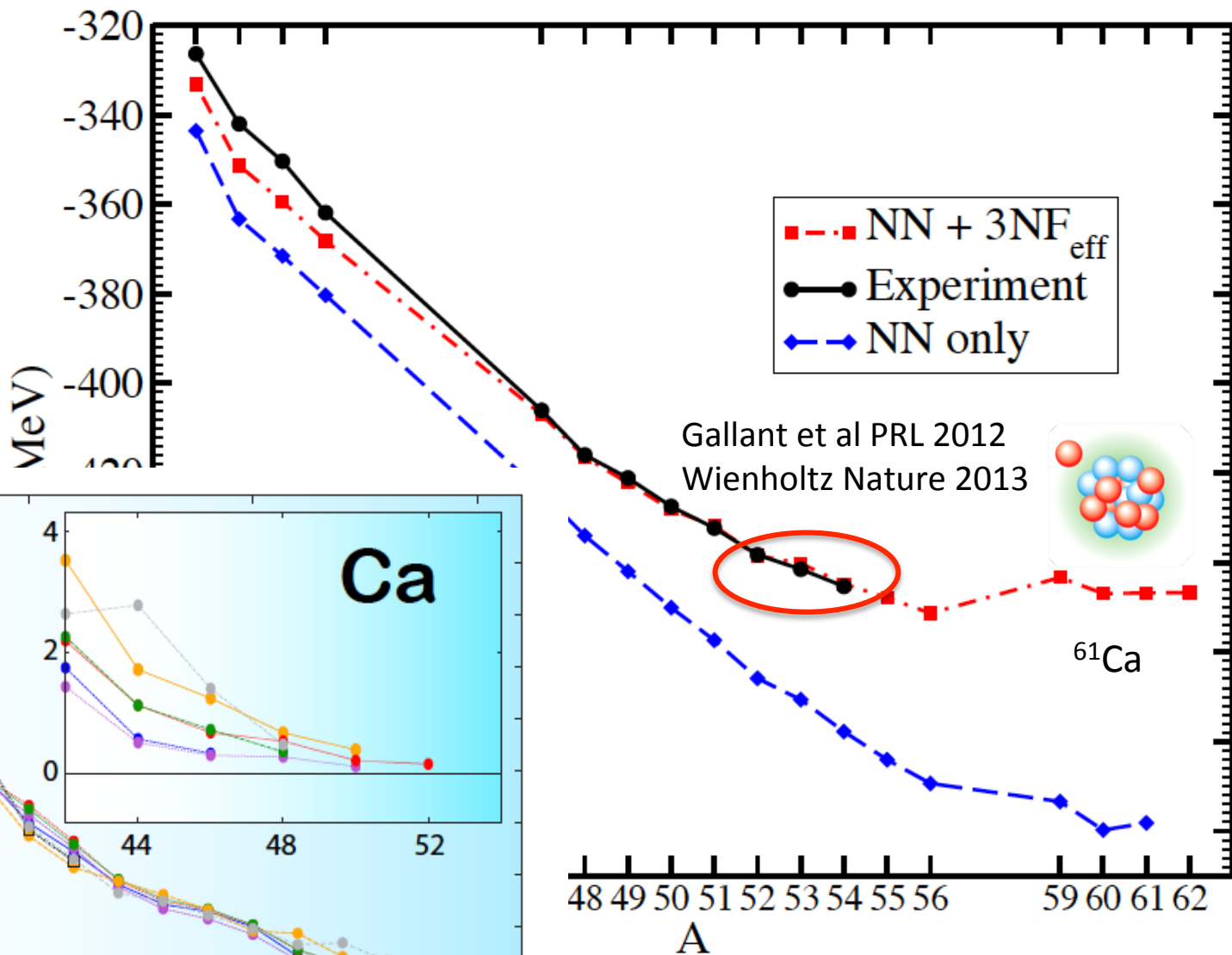


Neutron rich calcium isotopes

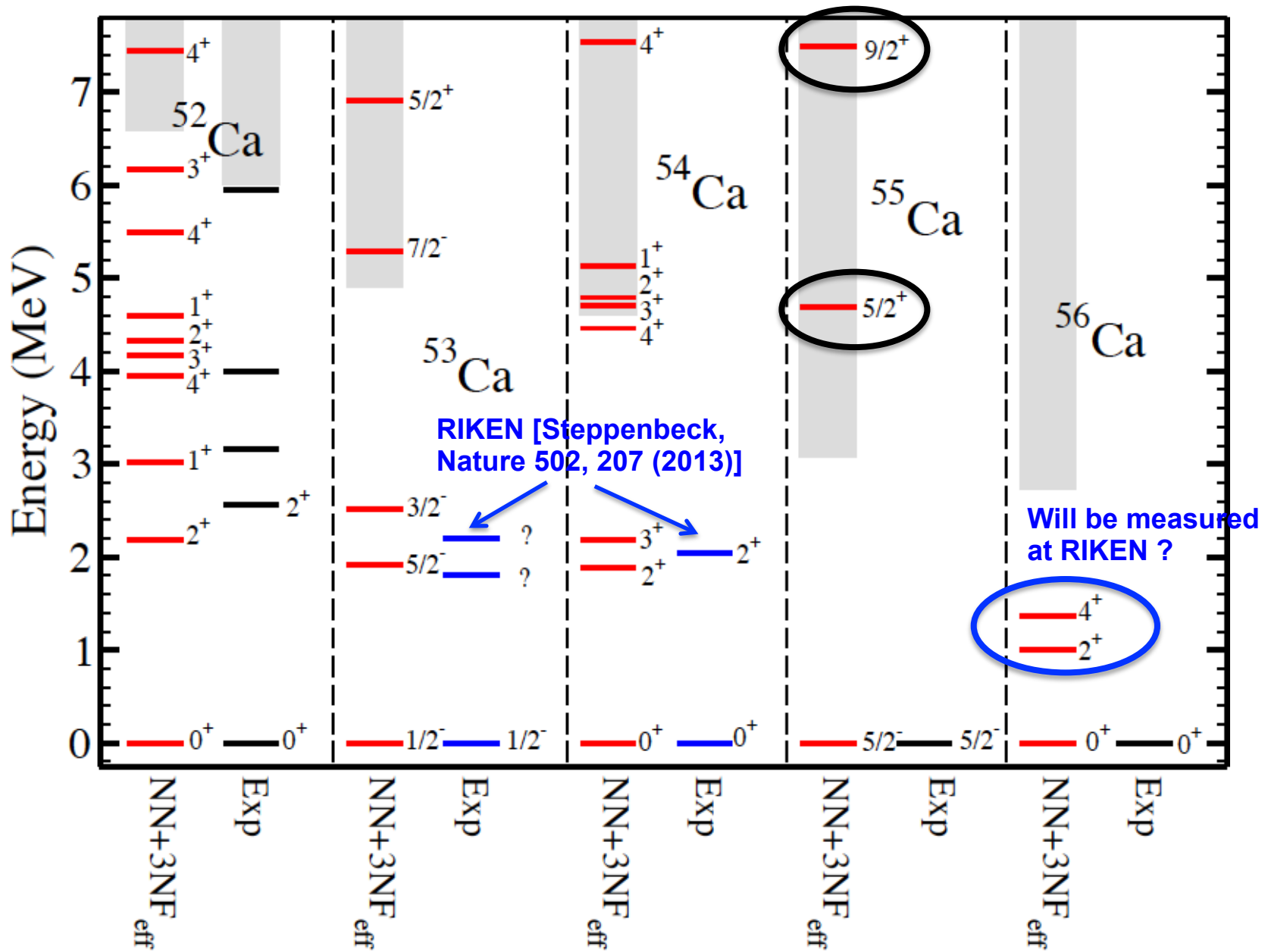
Hagen, Hjorth-Jensen, Jansen, Machleidt, Papenbrock, Phys. Rev. Lett. 109, 032502 (2012).

C Forssén et al
Phys. Scr. 014022 (2013)

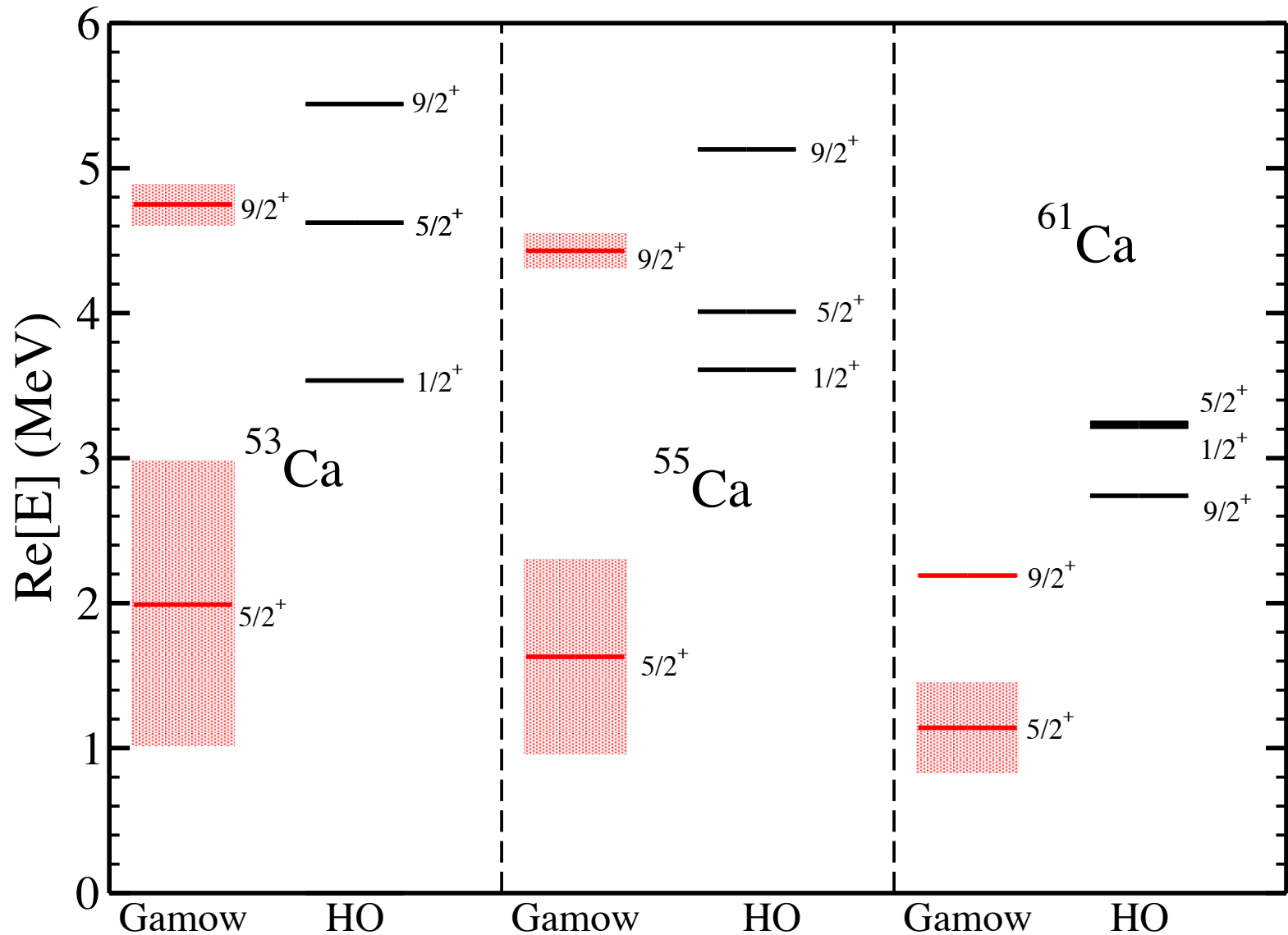
Erlér et al., Nature 486,
509 (2012)



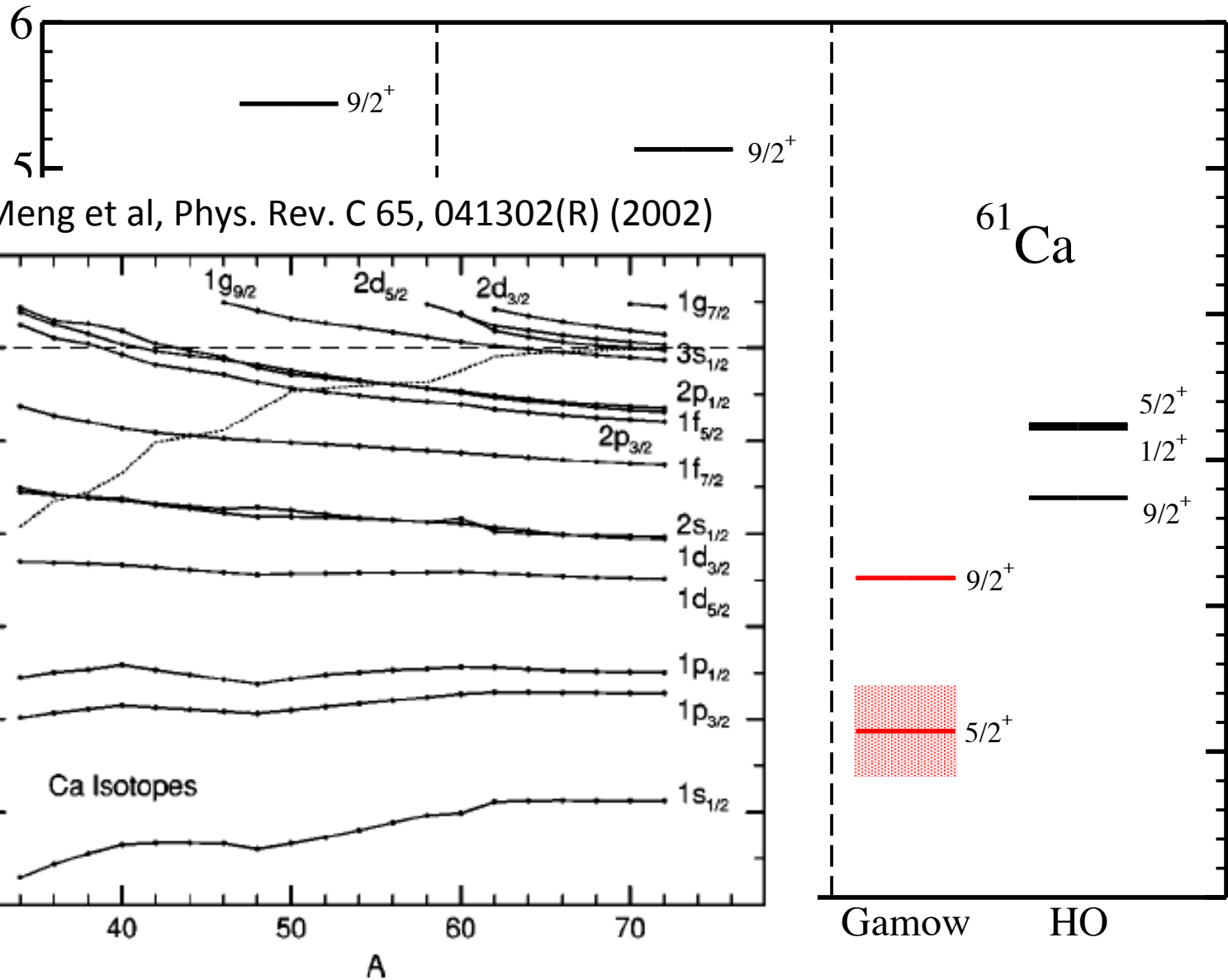
Spectra and shell evolution in Calcium isotopes



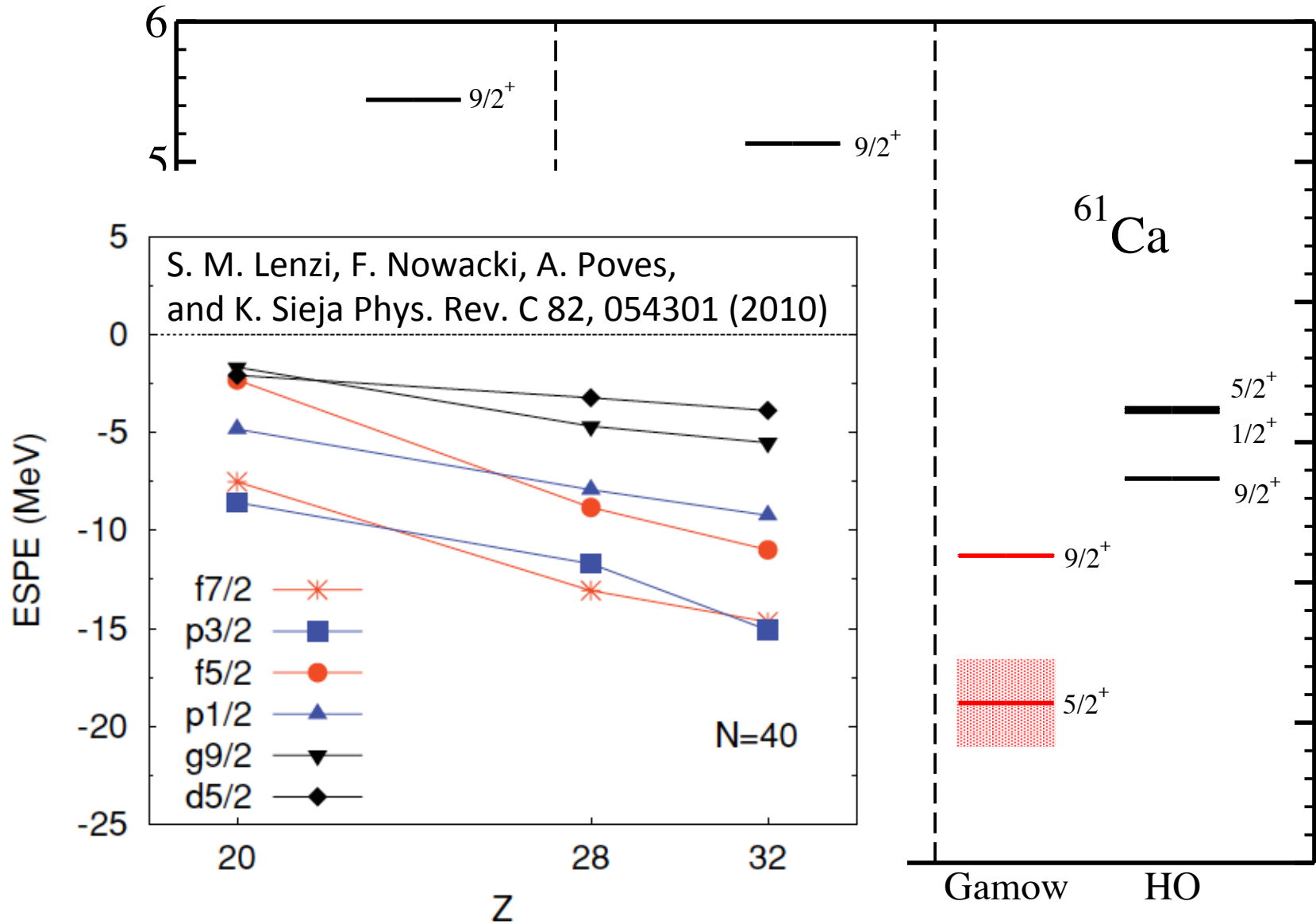
Effect of continuum on excited states in odd neutron rich Calcium isotopes



Effect of continuum on excited states in odd neutron rich Calcium isotopes



Effect of continuum on excited states in odd neutron rich Calcium isotopes



Towards nuclear reactions with coupled-cluster theory

One-nucleon overlap functions

Elastic scattering, capture and transfer reactions of a nucleon on/to a target nucleus with mass A is determined by the one-nucleon overlap function

$$O_A^{A+1}(lj; r) = \sum_n \langle A || a_{nlj} || A + 1 \rangle \phi_{nlj}(r)$$

The left ground-state for target nucleus A is given by: $\langle A | = \langle \Phi_0 | L_0 e^{-T}$

$$\langle \Phi_0 | L_0 e^{-T} H e^T = \langle \Phi_0 | L_0 \bar{H} = E_0 \langle \Phi_0 |$$

The A+1 final states are computed via particle-attached coupled-cluster method:

$$|A + 1\rangle = R^{A+1} e^T |\Phi_0\rangle = e^T \left(\sum_a r^a a_a^\dagger + \frac{1}{2} \sum_{abi} r_i^{ab} a_a^\dagger a_b^\dagger a_i \right) |\Phi_0\rangle$$

$$\bar{H} R^{A+1} |\Phi_0\rangle = E^{A+1} R^{A+1} |\Phi_0\rangle$$

Towards nuclear reactions with coupled-cluster theory

One-nucleon overlap function from coupled cluster theory:

Ø. Jensen et al PRC 82, 014310 (2010).

$$O_A^{A+1}(lj; r) = \sum_n \langle \Phi_0 | L_0 \overline{a}_{nlj} R^{A+1} | \Phi_0 \rangle \phi_{nlj}(r)$$

Bergren basis

ensures correct asymptotic behavior

The similarity transformed annihilation/creation operator calculated via the Baker-Campbell-Hausdorff commutator expansion:

$$\overline{a}_p = e^{-T} a_p e^T = [a_p, T]$$

$$\overline{a}_p = a_p + \sum_i t_i^p a_i + \frac{1}{2} \sum_{ijc} t_{ij}^{pc} a_c^\dagger a_j a_i$$

Treatment of long-range Coulomb effects

The A-nucleon Hamiltonian is:
$$\hat{H} = \sum_{1 \leq i < j \leq A} \left(\frac{(\vec{p}_i - \vec{p}_j)^2}{2mA} + \hat{V}_{NN}^{(i,j)} + \hat{V}_{\text{Coul}}^{(i,j)} + \hat{V}_{3\text{Neff}}^{(i,j)} \right)$$

We add and subtract a one-body Coulomb term:

$$V_{\text{Coul}} = U_{\text{Coul}}(r) + [V_{\text{Coul}} - U_{\text{Coul}}(r)]$$

$$U_{\text{Coul}}(r) \longrightarrow (Z - 1)e^2/r \text{ for } r \rightarrow +\infty$$

We construct the Coulomb Berggren basis by diagonalizing the 1-body Schrodinger equation
In a basis of spherical Bessel functions:

$$h = \frac{\hat{p}^2}{2m} - V_o \left[1 + \exp\left(\frac{r - R_0}{d}\right) \right]^{-1} + U_{\text{Coul}}(r)$$

Numerical example: proton resonances in ^{17}F
In a Woods-Saxon potential

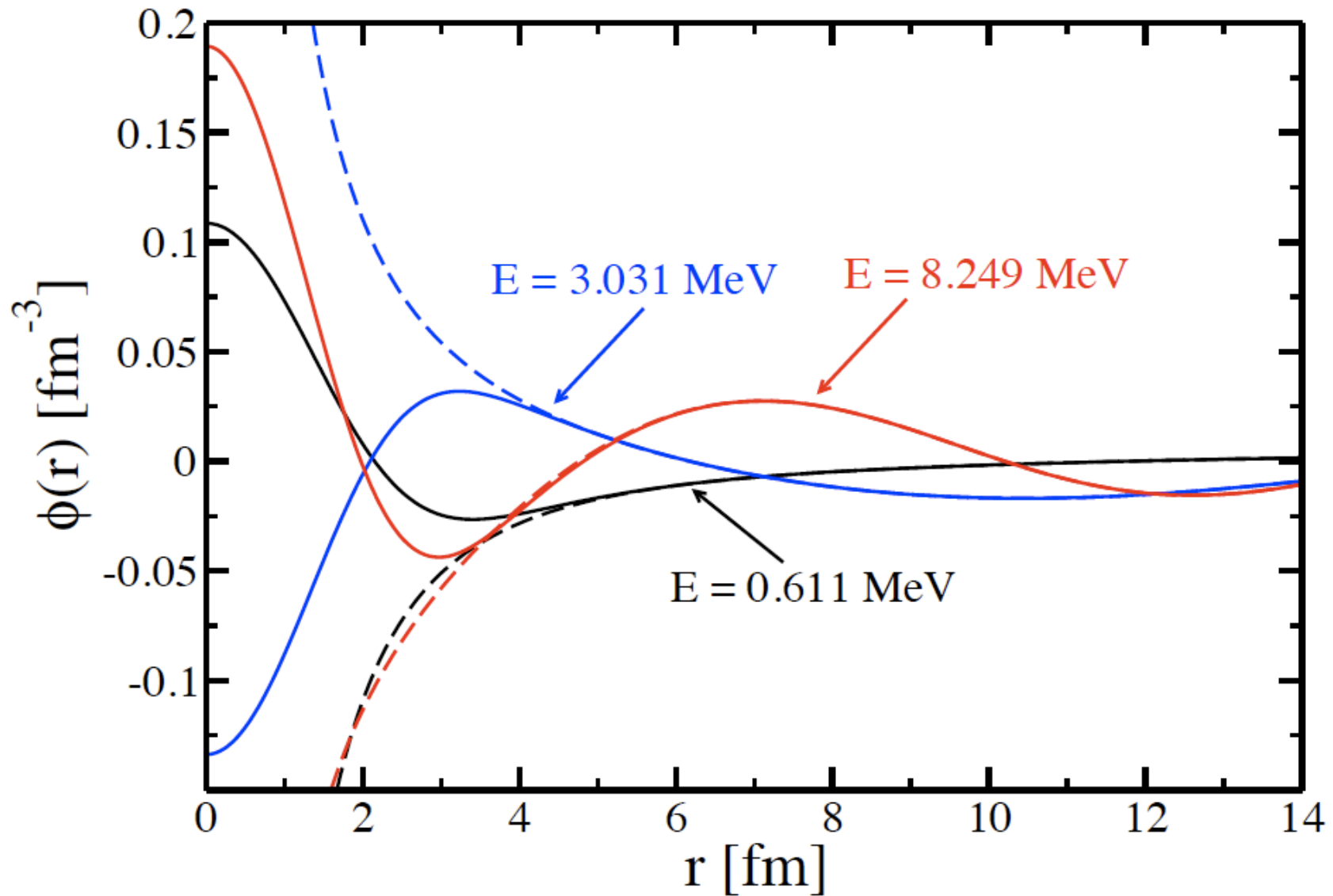
		$s_{1/2}$		$d_{3/2}$		$d_{5/2}$	
N_R	N_T	Re[E]	Γ	Re[E]	Γ	Re[E]	Γ
5	15	1.1054	0.1446	5.0832	1.3519	1.4923	0.0038
5	20	1.1033	0.1483	5.0785	1.3525	1.4873	0.0079
10	25	1.0989	0.1360	5.0765	1.3525	1.4858	0.0093
10	30	1.0986	0.1366	5.0757	1.3529	1.4849	0.0103
15	40	1.0978	0.1351	5.0749	1.3531	1.4842	0.0111
15	50	1.0978	0.1353	5.0746	1.3533	1.4838	0.0114
20	60	1.0976	0.1349	5.0745	1.3533	1.4837	0.0116
30	70	1.0975	0.1346	5.0744	1.3534	1.4837	0.0117
(Michel 2011)		1.0975	0.1346	5.0744	1.3535	1.4836	0.0119

The one-body coulomb potential has a Logarithmic singularity at $Q_\ell(1)$:

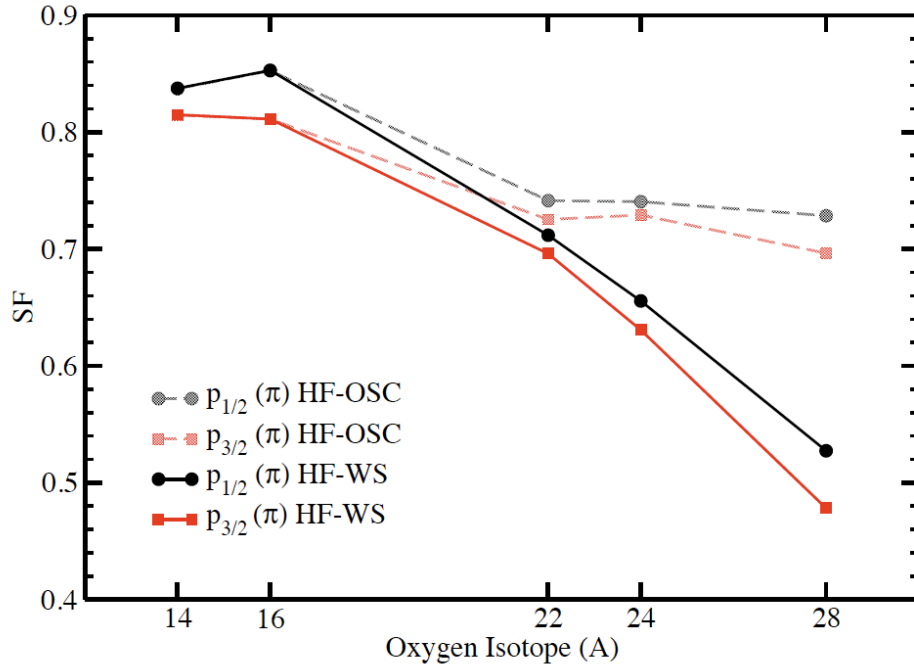
$$U_{\text{Coul}}(k, k') = \langle k | U_{\text{Coul}}(r) - \frac{(Z - 1)e^2}{r} | k' \rangle + \frac{(Z - 1)e^2}{\pi} Q_\ell \left(\frac{k^2 + k'^2}{2kk'} \right)$$

The singularity is removed by the **off-diagonal method**: replace the singularity by a finite value depending on the quadrature
N. Michel Phys. Rev. C 83, 034325 (2011)

Treatment of long-range Coulomb effects



Continuum induced correlations: Quenching of spectroscopic factors for proton removal in neutron rich oxygen isotopes



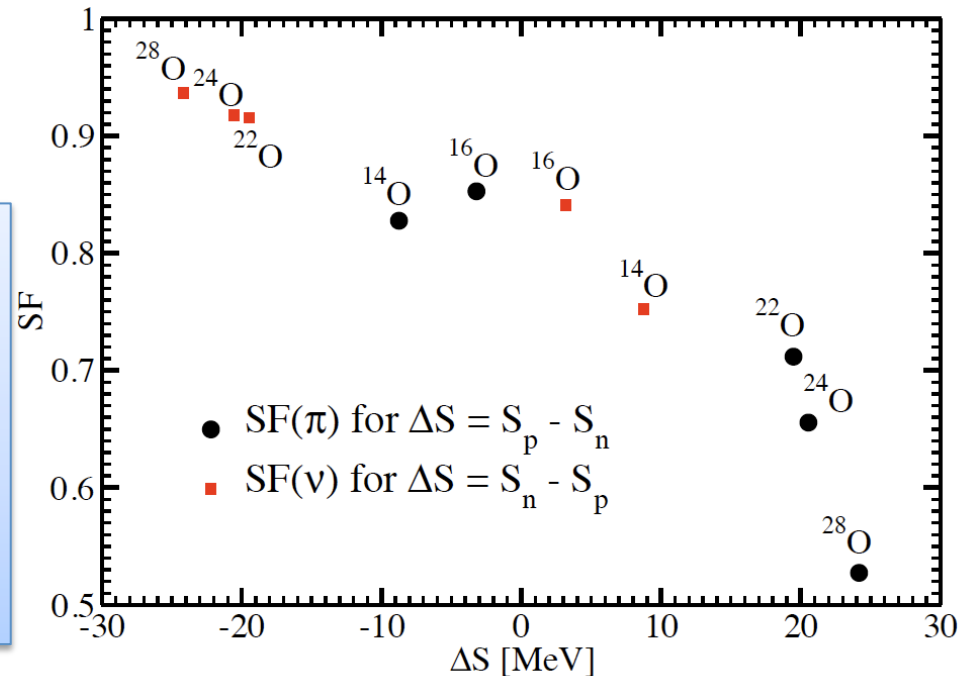
Spectroscopic factor is a useful tool to study correlations towards the dripline.

SF for proton removal in neutron rich ^{24}O show strong “quenching” pointing to large deviations from a mean-field like picture.

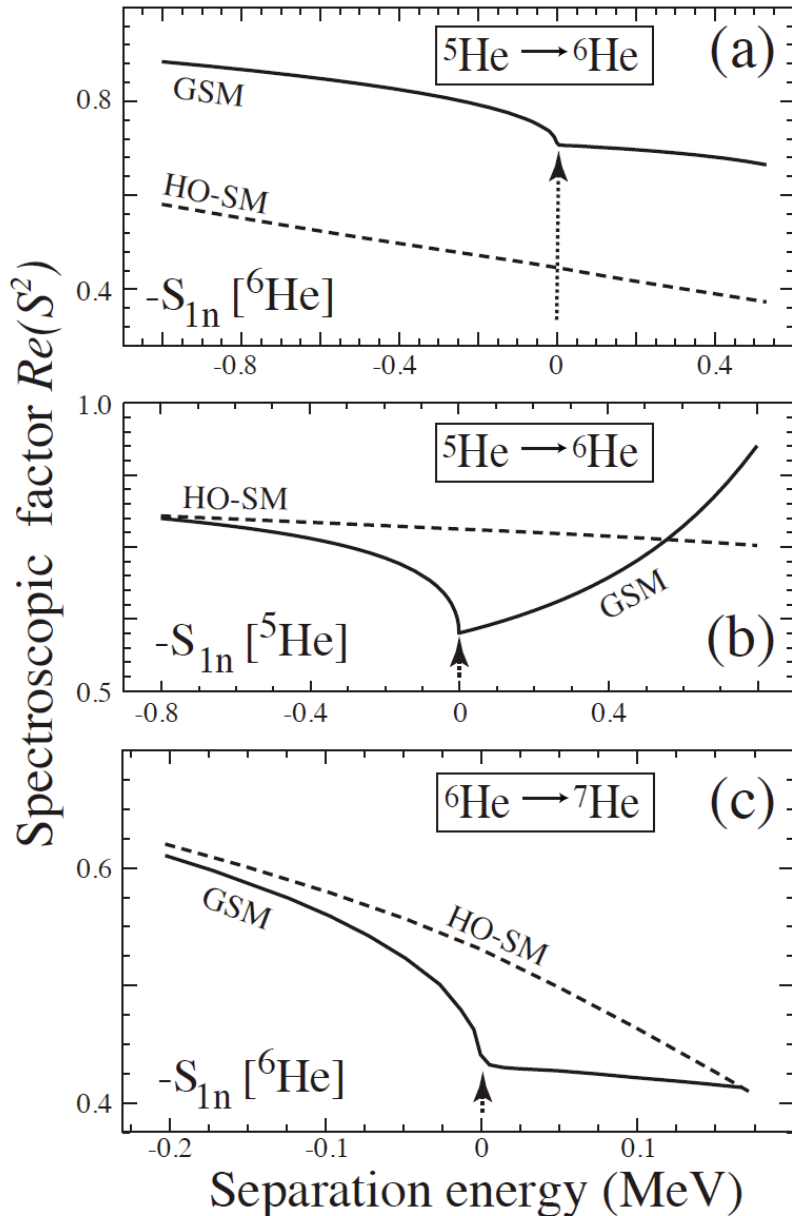
G. Hagen et al Phys. Rev. Lett. 107, 032501 (2011).

Strong asymmetry dependence on the SF for proton and neutron removal in neutron rich oxygen isotopes.

SF \sim 1 for neutron removal while protons are strongly correlated SF \sim 0.6-0.7 in $^{22,24,28}\text{O}$



Threshold effects and spectroscopic factors



Near the scattering threshold for one-neutron decay the spectroscopic factors are significantly influenced by the presence of the continuum. The standard shell model

$$\langle \Psi_A^{J_A} || a_{nlj}^+ || \Psi_{A-1}^{J_{A-1}} \rangle^2$$

approximation to spectroscopic factors completely fails in this region.

N. Michel et al Phys. Rev. C **75**, 031301 (2007)

N. Michel et al Nucl. Phys. A **794**, 29 (2007)

Top and middle:

$$\langle {}^6\text{He}(\text{g.s.}) || [{}^5\text{He}(\text{g.s.}) \otimes p_{3/2}]^{0^+} \rangle$$

Bottom :

$$\langle {}^7\text{He}(\text{g.s.}) || [{}^6\text{He}(\text{g.s.}) \otimes p_{3/2}]^{0^+} \rangle$$

Elastic proton/neutron scattering on ^{40}Ca

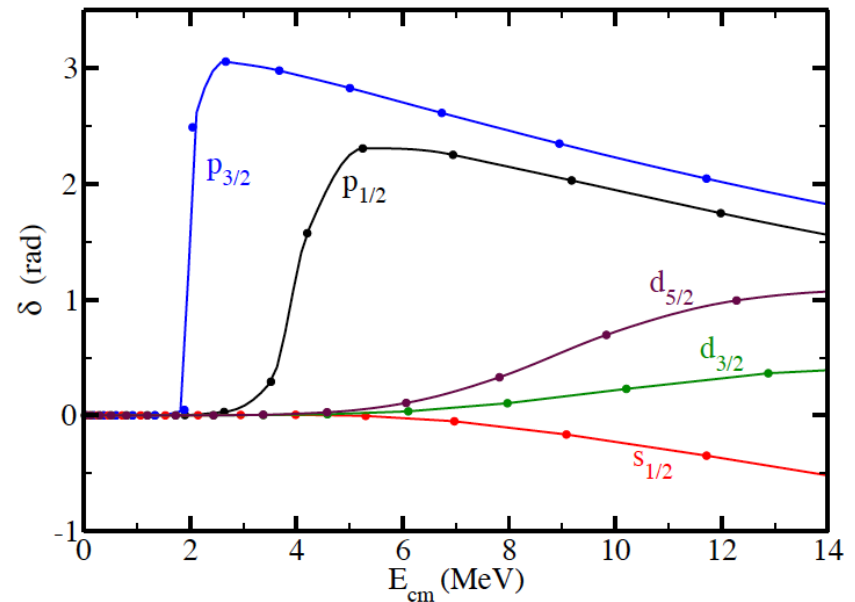
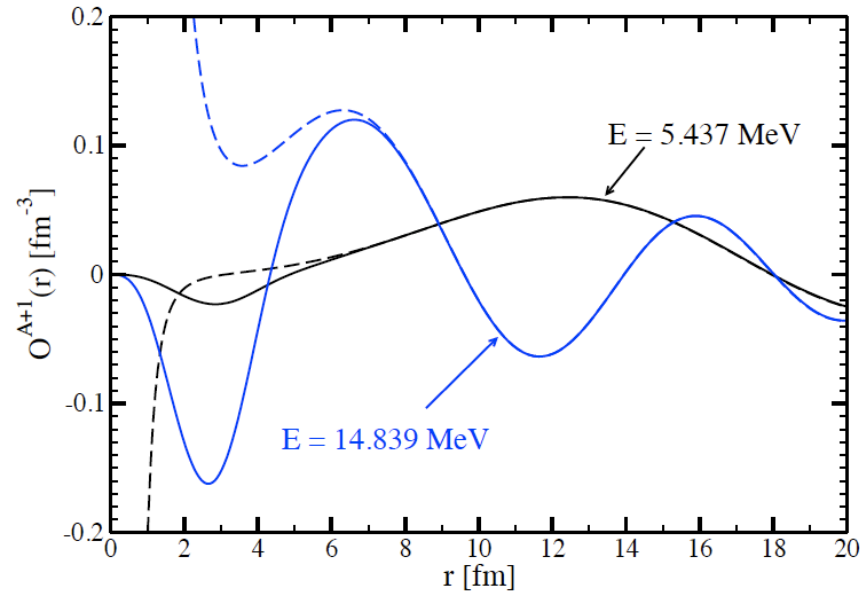
G. Hagen and N. Michel, Phys. Rev. C 86, 021602(R) (2012).

The one-nucleon overlap function: $O_A^{A+1}(lj; r) = \sum_n \langle A || a_{nlj} || A + 1 \rangle \phi_{nlj}(r)$

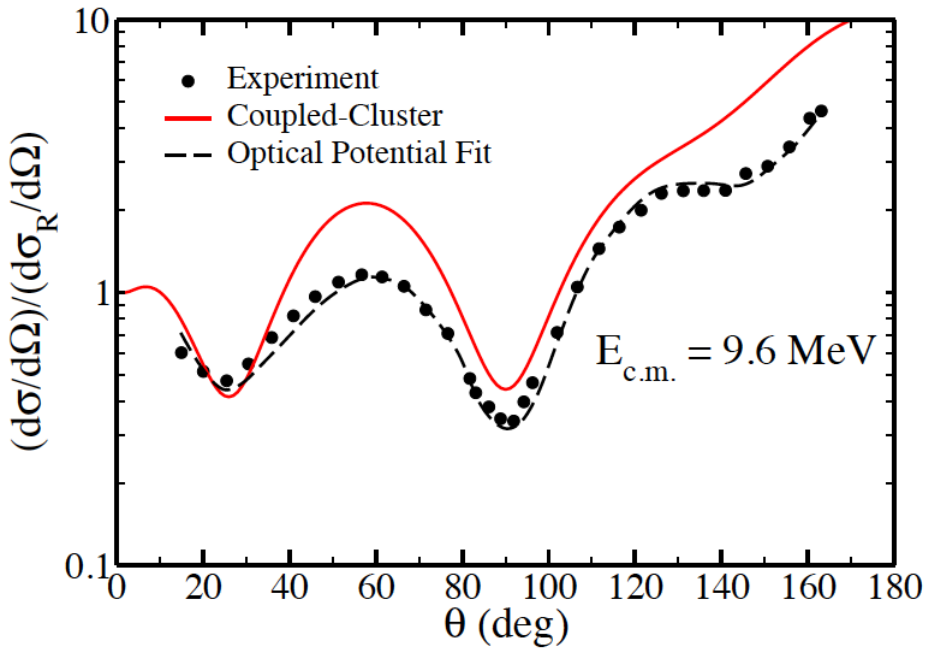
Beyond the range of the nuclear interaction the overlap functions take the form:

$$O_A^{A+1}(lj; kr) = C_{lj} \frac{W_{-\eta, l+1/2}(kr)}{r}, \quad k = i\kappa$$

$$O_A^{A+1}(lj; kr) = C_{lj} [F_{\ell, \eta}(kr) - \tan \delta_l(k) G_{\ell, \eta}(kr)]$$



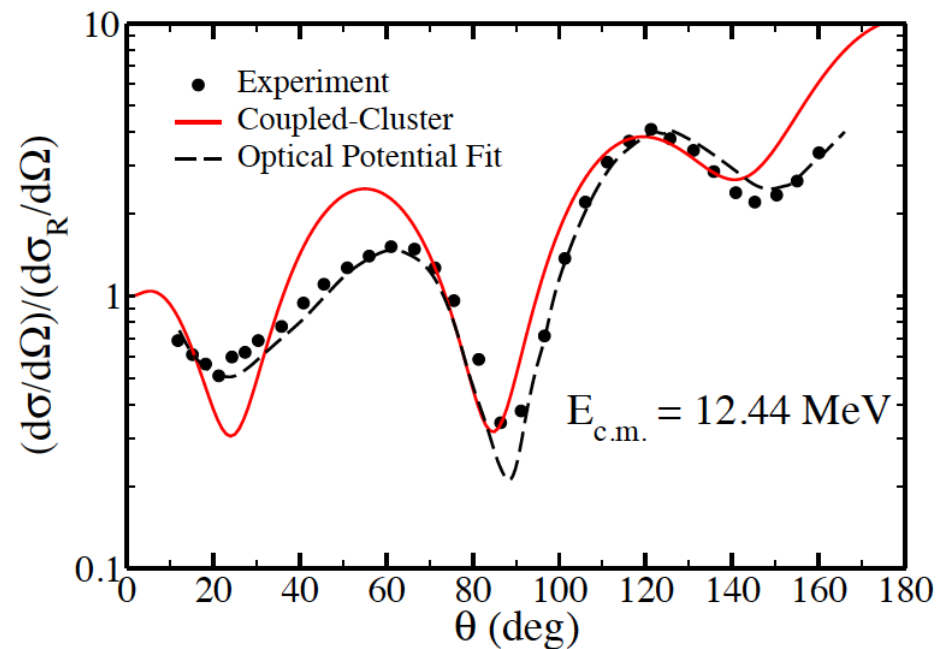
Elastic proton/neutron scattering on ^{40}Ca



Differential cross section for elastic proton scattering on ^{40}Ca .

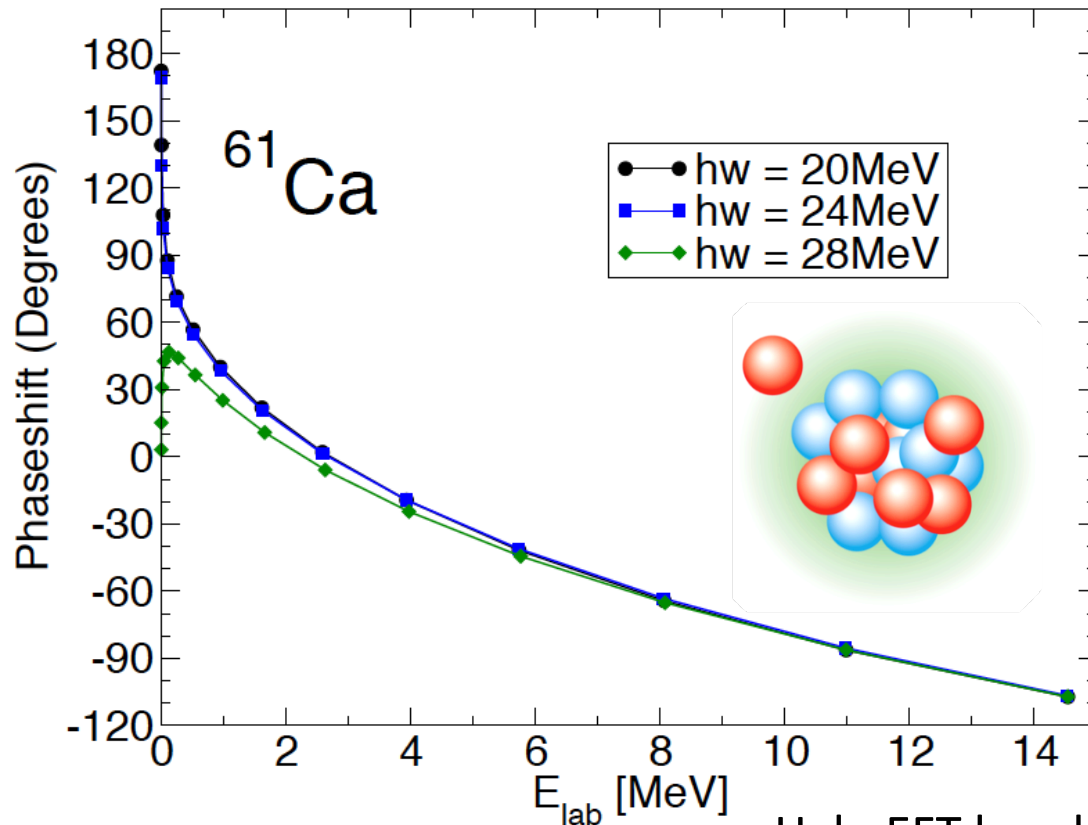
Fair agreement between theory and experiment for low-energy scattering.

G. Hagen and N. Michel
Phys. Rev. C **86**, 021602(R) (2012).



Efimov physics around neutron rich ^{60}Ca

G. Hagen, P. Hagen, H.-W. Hammer, and L. Platter, PRL 111, 132501 (2013)



- Phase shifts from CC overlap functions
- Large S-wave scattering length in ^{61}Ca implies Halo phenomena
- Novel Approach: Merge halo-EFT and input from CC to study properties of ^{62}Ca

Halo EFT breakdown scale

$\hbar\omega$ [MeV]	a_{cn} [fm]	r_{cn} [fm]	S_n [keV]	S_{deep} [keV]
20	55.0	8.8	8.4	544
24	53.2	9.1	5.3	509
28	-26.1	10.8	-	361

	^{53}Ca		^{55}Ca		^{61}Ca	
J^π	Re[E]	Γ	Re[E]	Γ	Re[E]	Γ
$5/2^+$	1.99	1.97	1.63	1.33	1.14	0.62
$9/2^+$	4.75	0.28	4.43	0.23	2.19	0.02

Efimov physics around neutron rich ^{60}Ca

- Halo EFT provides a model-independent description of halo nuclei
- Core + valence nucleons are effective degrees of freedom
- The coupling constants from the n - n and core- n effective range
- The expansion is given in powers of R/a with $R \sim$ effective range
- Use coupled-cluster results for ^{61}Ca to study signals of Efimov physics

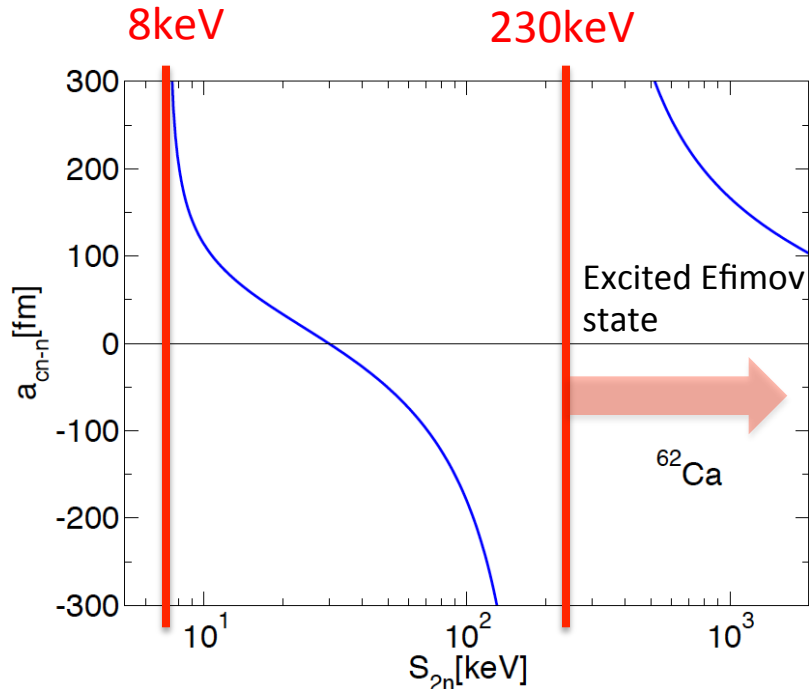
The Halo EFT core n - n Lagrangian to leading order:

$$\begin{aligned}
 \mathcal{L} = & \psi_c^\dagger \left(i\partial_0 + \frac{\vec{\nabla}^2}{2M} \right) \psi_c + \vec{\psi}_n^\dagger \left(i\partial_0 + \frac{\vec{\nabla}^2}{2m} \right) \vec{\psi}_n \\
 & + \Delta_{nn} d_{nn}^\dagger d_{nn} + \Delta_{cn} \vec{d}_{cn}^\dagger \vec{d}_{cn} + h d_{nn}^\dagger \psi_c^\dagger \psi_c d_{nn} \\
 & - \left[g_{cn} \vec{d}_{cn}^\dagger \vec{\psi}_n \psi_c + \frac{g_{nn}}{2} d_{nn}^\dagger (\vec{\psi}_n^T P \vec{\psi}_n) + \text{h.c.} \right] + \dots
 \end{aligned}$$

Coupling constants given by n - n and core- n effective ranges

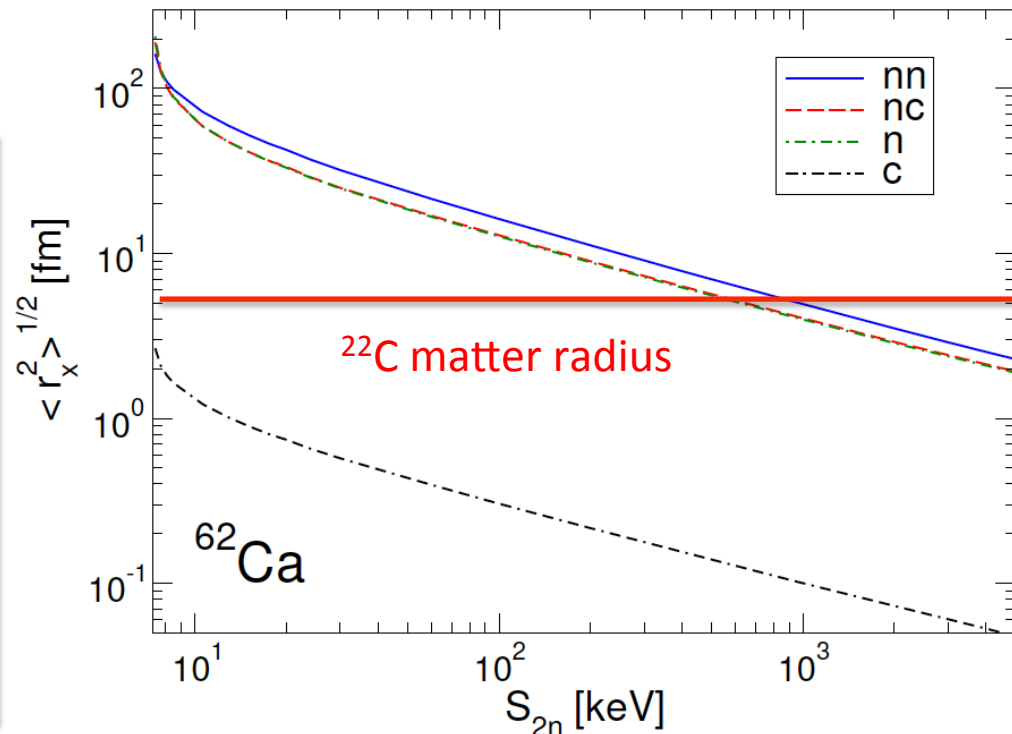
Three-body coupling

Efimov physics around neutron rich ^{60}Ca

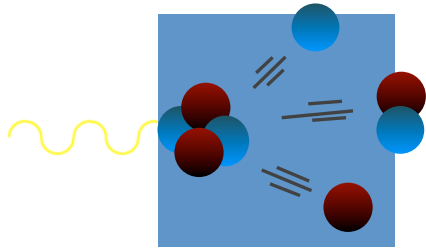


- For S_{2n} larger than $\sim 230\text{keV}$ another state appears in the spectrum
- ^{62}Ca is likely to have an Efimov state (large halo)
- It is conceivable that ^{62}Ca displays an excited Efimov state

- ^{22}C is the largest known two-neutron halo $R_{\text{rms}} \sim 5.4\text{fm}$ (Tanaka PRL 2010)
- Computed matter radii for ^{62}Ca indicates that it has the potential to be the largest and heaviest halo in the chart of nuclei



Break-up observables for medium-mass nuclei



Cross section is related to the Response Function in the continuum

$$S(\omega) = \sum_f \left| \langle \psi_f | \hat{O} | \psi_0 \rangle \right|^2 \delta(E_f - E_0 - \omega)$$

Cannot be calculated beyond 3-body break-up even for A=4

Solution: Lorentz Integral Transform method
(Efros, Leidemann, Orlandini, Barnea, Bacca)

Efros *et al.*, J. Phys. G: Nucl. Part. Phys. 34 (2007)

$$\mathcal{L}(\sigma, \Gamma) = \int d\omega \frac{S(\omega)}{(\omega - \sigma)^2 + \Gamma^2} = \langle \tilde{\Psi} | \tilde{\Psi} \rangle$$

$$(H - E_0 - \sigma + i\Gamma) |\tilde{\Psi}\rangle = O|\Psi_0\rangle$$

Bound-state-like object. Need bound state technique to calculate it

$$\underbrace{R(z^*) e^T}_{\text{Lorentz Integral Transform}} |\Phi_0\rangle = e^T \left(\sum_{ia} r_a^i a_a^\dagger a_i + \frac{1}{4} \sum_{abij} r_{ij}^{ab} a_a^\dagger a_b^\dagger a_j a_i \right) |\Phi_0\rangle$$

Coupled-cluster formulation of the Lorentz-Integral Transformation

Want to solve the Schrödinger like equation with a source term: $(H - E_0 - \sigma + i\Gamma) |\tilde{\Psi}\rangle = O|\Phi_0\rangle$

$|\tilde{\Psi}\rangle$ Solve via Equation Of Motion (EOM):

$$\underbrace{R(z^*)e^T|\Phi_0\rangle}_{|\tilde{\Psi}\rangle} = e^T \left(\sum_{ia} r_a^i a_a^\dagger a_i + \frac{1}{4} \sum_{abij} r_{ij}^{ab} a_a^\dagger a_b^\dagger a_j a_i \right) |\Phi_0\rangle$$

By using the right and left EOM ansatz for $\tilde{\Psi}$ we can write down right/left EOM equations

Use BCH commutator expansion to compute similarity transforms:

$$(\bar{H} - E_0 - \sigma + i\Gamma) R|\Phi_0\rangle = \bar{O}|\Phi_0\rangle$$

$$\langle\Phi_0|\tilde{L}(\bar{H} - E_0 - \sigma - i\Gamma) = \langle\Phi_0|L_0\bar{O}^\dagger$$

$$\bar{O} = e^{-T} O e^T,$$

$$\bar{O}^\dagger = e^{-T} O^\dagger e^T$$

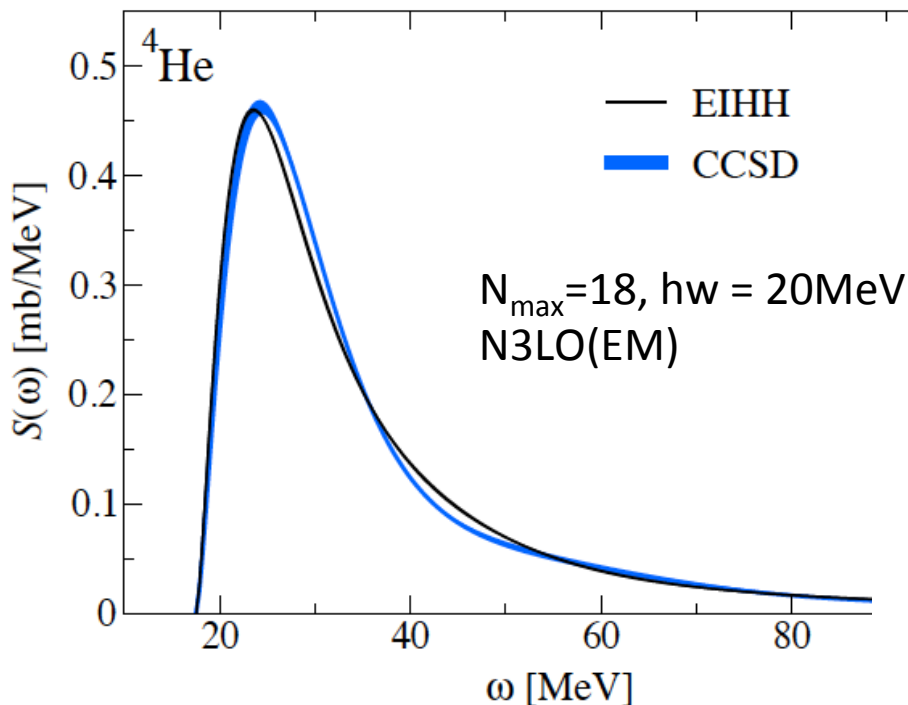
The Lorentz-Integral

Transformaiton is then given: $\mathcal{L}(\sigma, \Gamma) = \langle\Phi_0|\tilde{L}(z)R(z^*)|\Phi_0\rangle$

Dipole response in ^4He from coupled-cluster

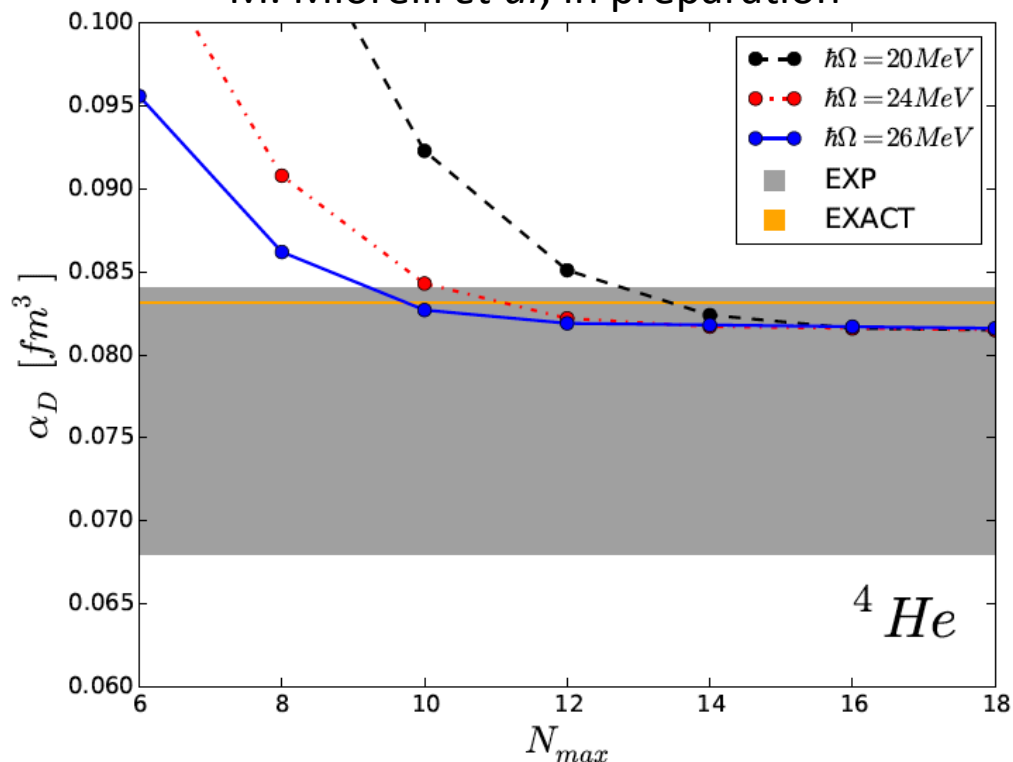
S. Bacca, N. Barnea, G. Hagen, G. Orlandini, T. Papenbrock, PRL 111, 143402 (2013).

S. Bacca, N. Barnea, G. Hagen, M. Miorelli, G. Orlandini, T. Papenbrock, PRC 90, 064610 (2014)



Lorentz Integral transform from coupled-cluster benchmarked with “exact” hyper-spherical harmonics for ^4He

M. Miorelli *et al*, in preparation



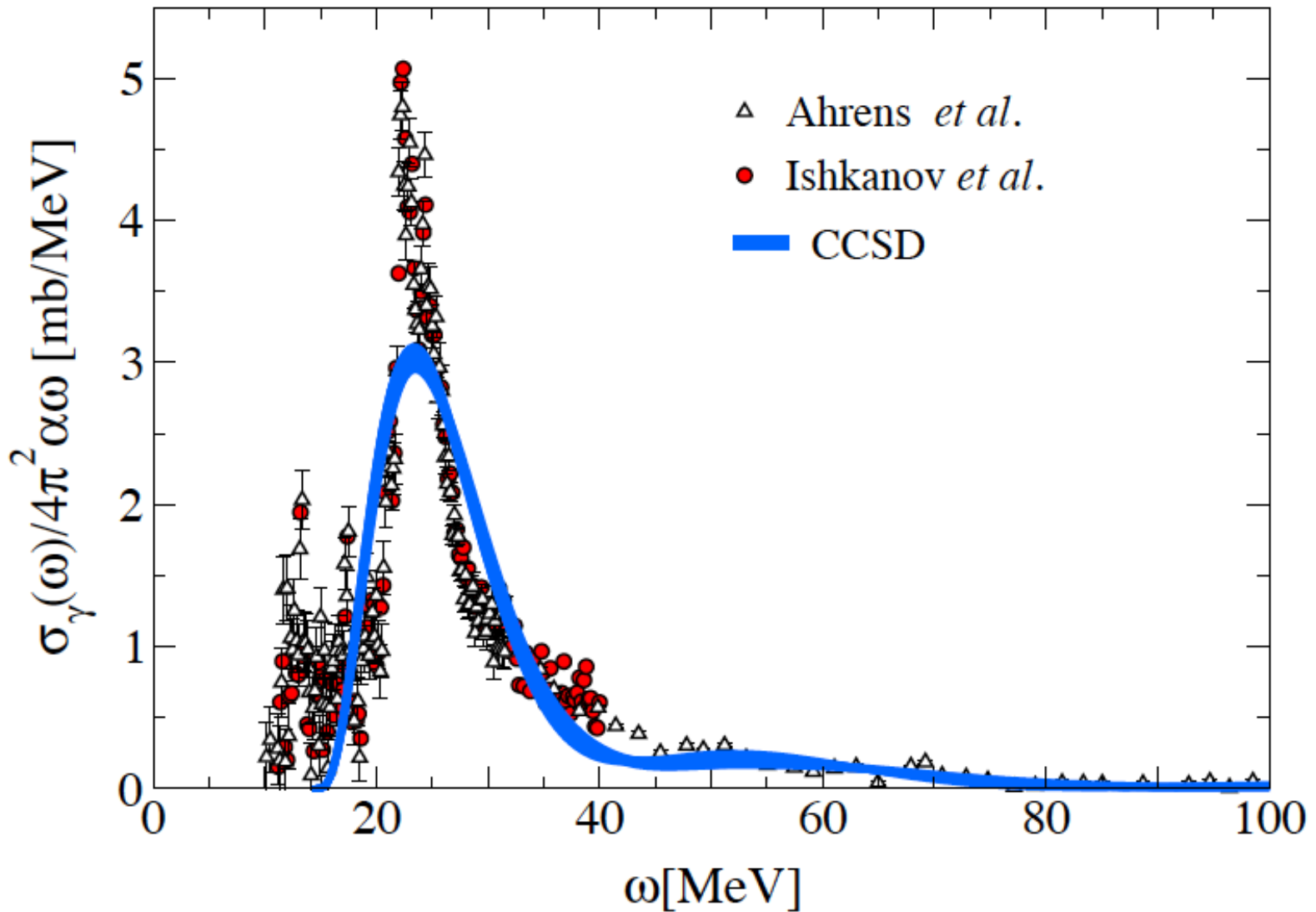
Dipole polarizability in ^4He from CCSD within 1% of exact Hyper-spherical harmonics

$$\alpha_D = 2\alpha \int_{\omega_{\text{th}}}^{\infty} d\omega \frac{S(\omega)}{\omega}$$

Giant dipole resonance in ^{16}O

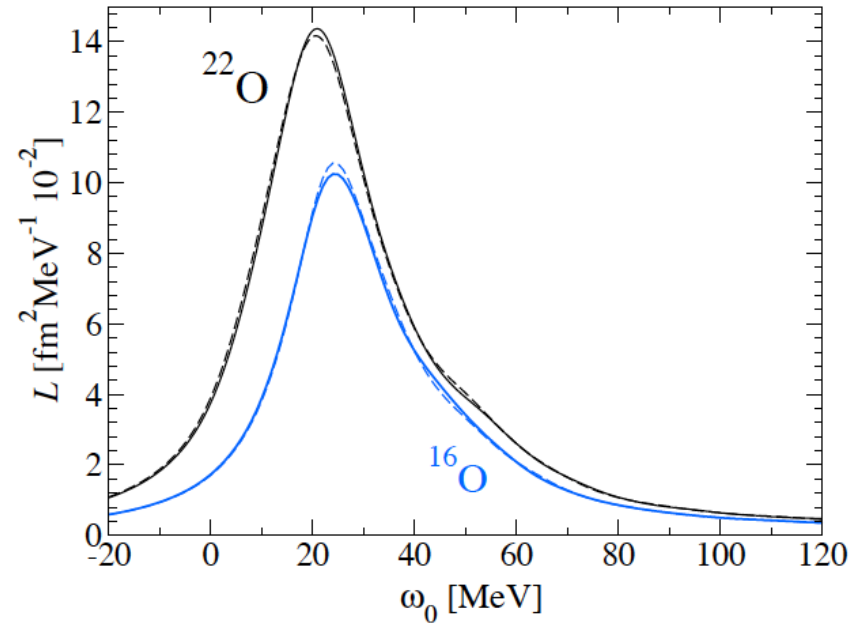
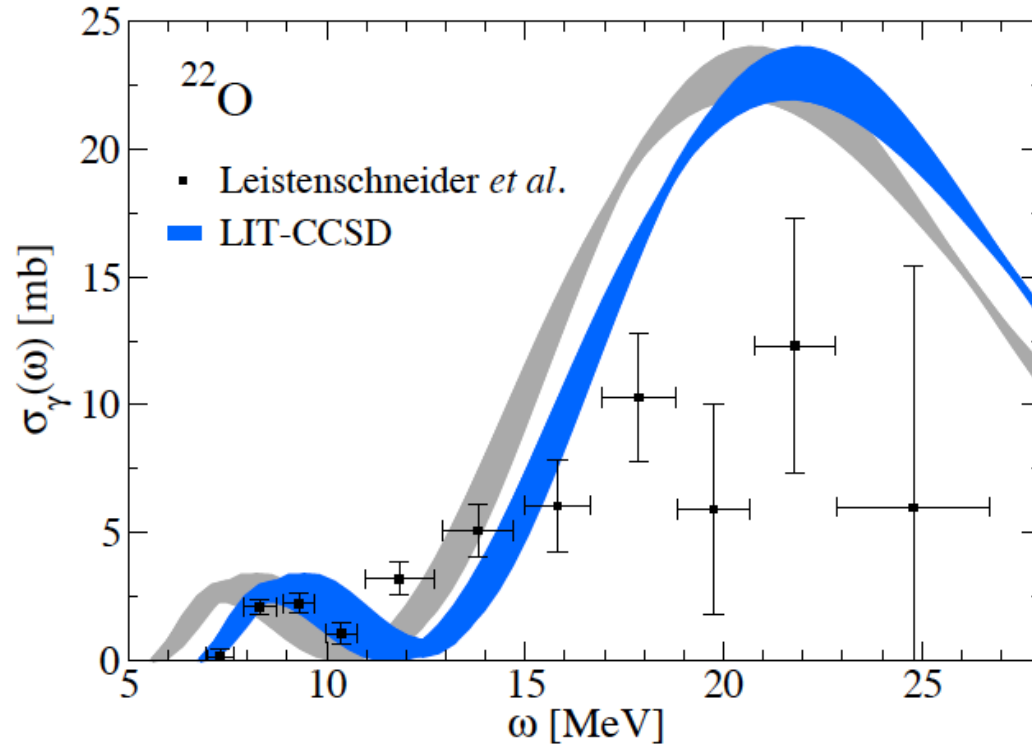
N^3LO Entem & Machleidt (NN only)

S. Bacca, N. Barnea, G. Hagen, G. Orlandini, T. Papenbrock, PRL 111, 143402 (2013).



Dipole response in ^{22}O

S. Bacca, N. Barnea, G. Hagen, M. Miorelli, G. Orlandini, T. Papenbrock, PRC 90, 064610 (2014)



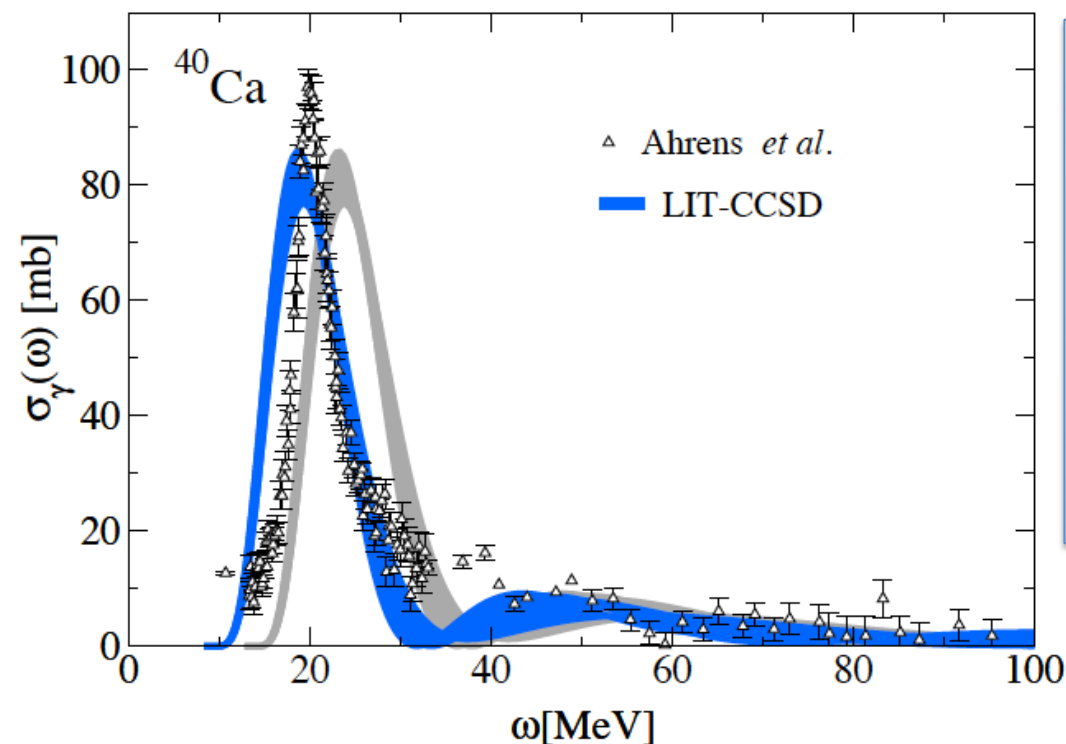
$$\text{BSR} \equiv \int_{\omega_{\text{th}}}^{\infty} d\omega S(\omega) = \langle 0 | \hat{D}_0^\dagger \hat{D}_0 | 0 \rangle$$

$$\text{BSR} \propto \left(\frac{NZ}{A} \right)^2 R_{PN}^2$$

We find low-lying dipole strength consistent with experiment
Total dipole strength is enhanced in ^{22}O as compared to ^{16}O which can be explained by the excess of neutrons in ^{22}O

Dipole response and polarizability in ^{40}Ca

N³LO Entem & Machleidt (NN only)



- Dipole response in ^{40}Ca compared to data.
- Dipole resonance at too high energy, implies too small electric dipole polarizability.

$$\alpha_D(\text{Th}) = 1.47 \text{ fm}^3$$

$$\alpha_D(\text{Exp}) = 2.23(3) \text{ fm}^3$$

$$R_{\text{ch}}(\text{Th}) = 3.05 \text{ fm}$$

$$R_{\text{ch}}(\text{Exp}) = 3.48 \text{ fm}$$

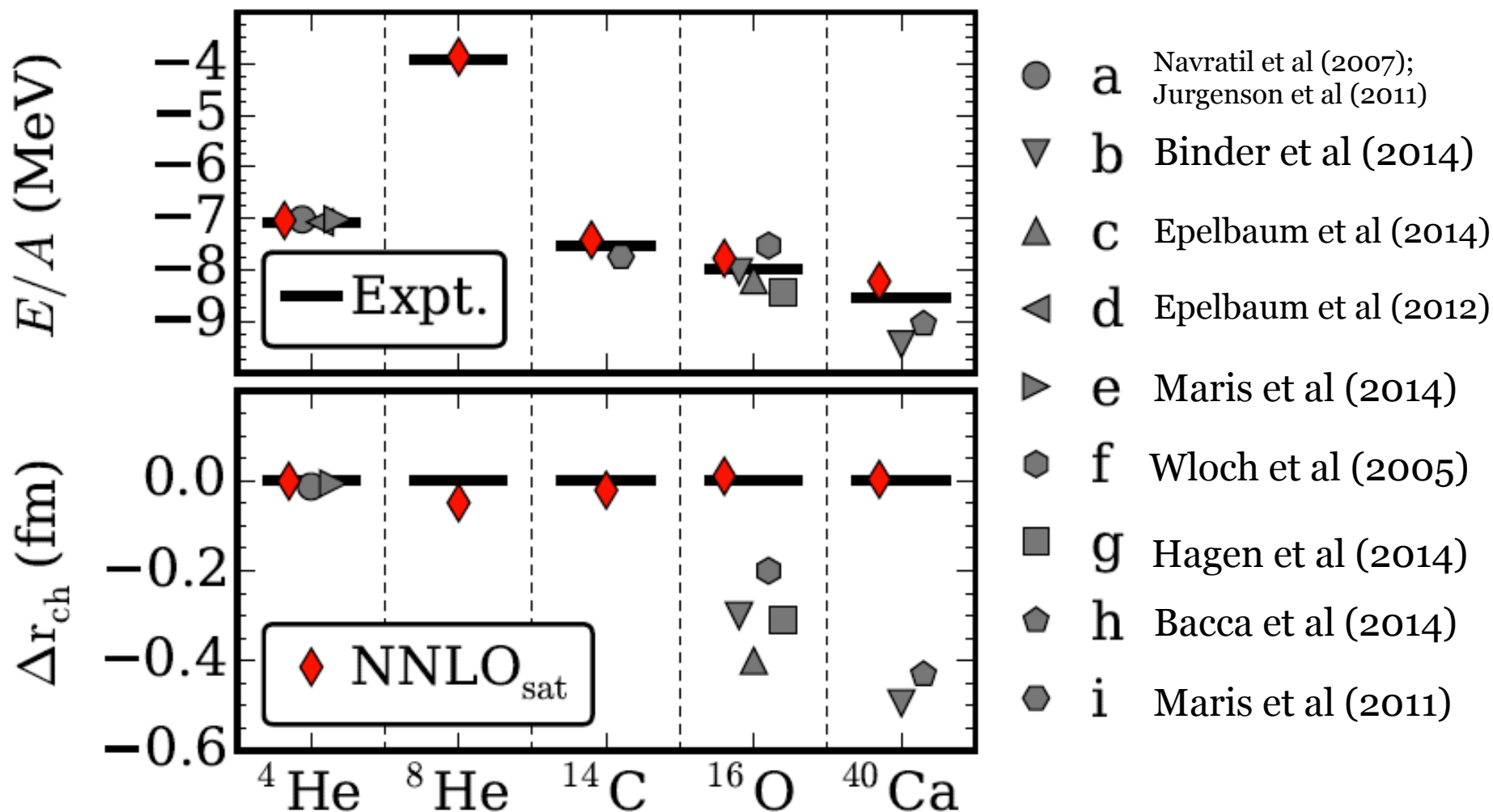
$$E(\text{Th}) = 362 \text{ MeV}$$

$$E(\text{Exp}) = 342 \text{ MeV}$$

Current chiral interactions do not have good saturation properties. Radii and binding energies are off the experimental target values

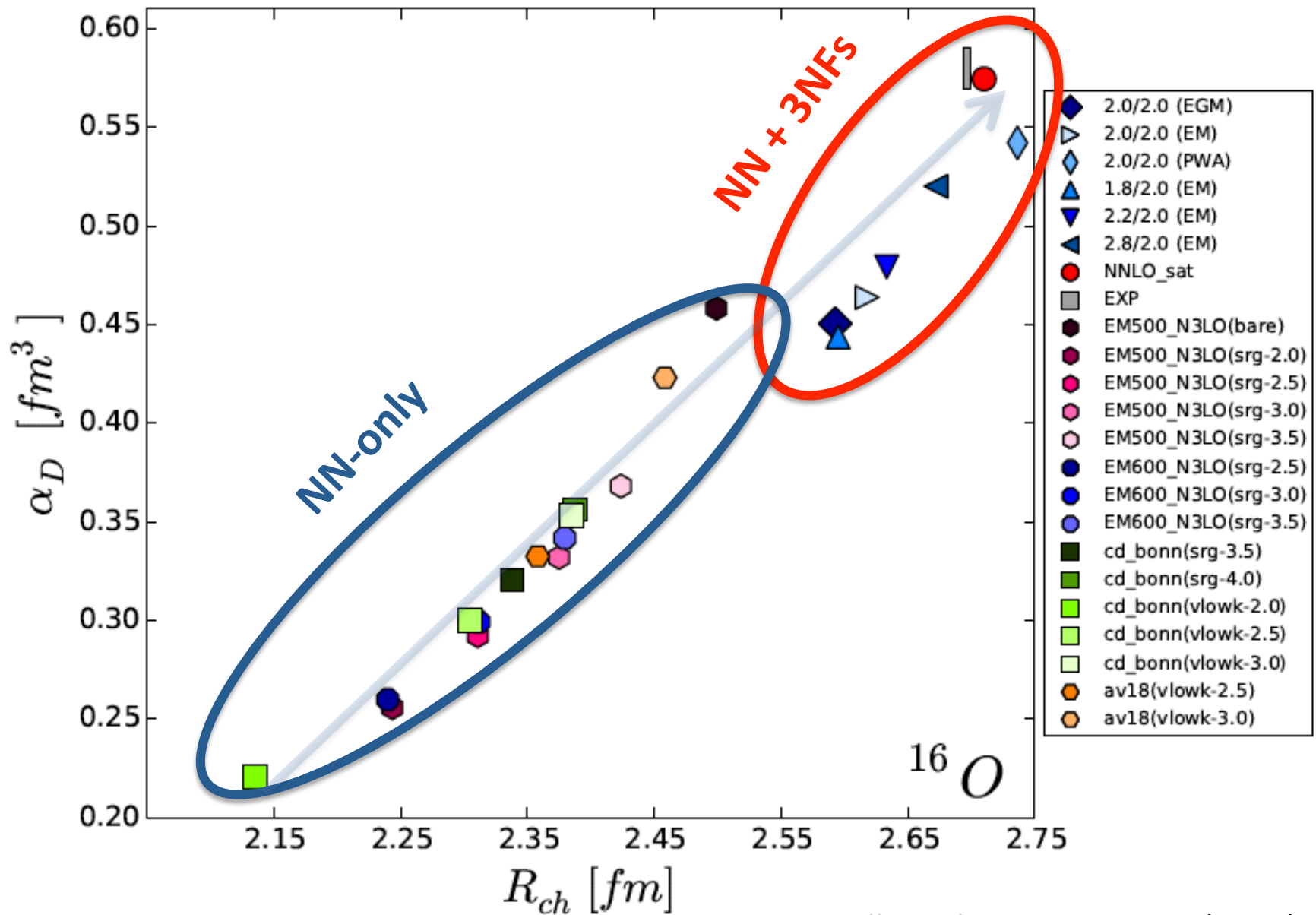
How to solve the problem of saturation?

Accurate nuclear binding energies and radii from a chiral interaction



Our solution: simultaneous optimization of NN and 3NFs with input from selected nuclei up to $A \sim 25$ (NNLO_{sat}). A. Ekström *et al*, Phys. Rev. C **91**, 051301(R) (2015)

Dipole polarizability of ^{16}O



Backup slides

Detection of neutron clusters

F. M. Marqués,^{1,*} M. Labiche,^{1,†} N. A. Orr,¹ J. C. Angélique,¹ L. Axelsson,² B. Benoit,³ U. C. Bergmann,⁴ M. J. G. Borge,⁵ W. N. Catford,⁶ S. P. G. Chappell,⁷ N. M. Clarke,⁸ G. Costa,⁹ N. Curtis,^{6,‡} A. D'Arrigo,³ E. de Góes Brennand,³ F. de Oliveira Santos,¹⁰ O. Dorvaux,⁹ G. Fazio,¹¹ M. Freer,^{8,1} B. R. Fulton,^{8,§} G. Giardina,¹¹ S. Grévy,^{12,||} D. Guillemaud-Mueller,¹² F. Hanappe,³ B. Heusch,⁹ B. Jonson,² C. Le Brun,^{1,¶} S. Leenhardt,¹² M. Lewitowicz,¹⁰ M. J. López,^{10,**} K. Markenroth,² A. C. Mueller,¹² T. Nilsson,^{2,††} A. Ninane,^{1,‡‡} G. Nyman,¹ I. Piqueras,⁵ K. Riisager,⁴ M. G. Saint Laurent,¹⁰ F. Sarazin,^{10,§§} S. M. Singer,⁸ O. Sorlin,¹² and L. Stuttgé⁹

¹*Laboratoire de Physique Corpusculaire, IN2P3-CNRS, ISMRa et Université de Caen, F-14050 Caen Cedex, France*

²*Experimentell Fysik, Chalmers Tekniska Högskola, S-412 96 Göteborg, Sweden*

³*Université Libre de Bruxelles, CP 226, B-1050 Bruxelles, Belgium*

⁴*Institut for Fysik og Astronomi, Aarhus Universitet, DK-8000 Aarhus C, Denmark*

⁵*Instituto de Estructura de la Materia, CSIC, E-28006 Madrid, Spain*

⁶*Department of Physics, University of Surrey, Guildford, Surrey GU2 7XH, United Kingdom*

⁷*Department of Nuclear Physics, University of Oxford, Keble Road, Oxford OX1 3RH, United Kingdom*

⁸*School of Physics and Astronomy, University of Birmingham, Birmingham B15 2TT, United Kingdom*

⁹*Institut de Recherche Subatomique, IN2P3-CNRS, Université Louis Pasteur, BP 28, F-67037 Strasbourg Cedex, France*

¹⁰*GANIL, CEA/DSM-CNRS/IN2P3, BP 55027, F-14076 Caen Cedex, France*

¹¹*Dipartimento di Fisica, Università di Messina, Salita Sperone 31, I-98166 Messina, Italy*

¹²*Institut de Physique Nucléaire, IN2P3-CNRS, F-91406 Orsay Cedex, France*

(Received 27 November 2001; published 1 April 2002)

A new approach to the production and detection of bound neutron clusters is presented. The technique is based on the breakup of beams of very neutron-rich nuclei and the subsequent detection of the recoiling proton in a liquid scintillator. The method has been tested in the breakup of intermediate energy (30–50 MeV/nucleon) ¹¹Li, ¹⁴Be, and ¹⁵B beams. Some six events were observed that exhibit the characteristics of a multineutron cluster liberated in the breakup of ¹⁴Be, most probably in the channel ¹⁰Be+⁴n. The various backgrounds that may mimic such a signal are discussed in detail.

NewScientist

The global science and technology weekly | 16 October 2002

NEW! US JOBS SECTION

ELEMENT ZERO?

Theory says it can't exist,
but experiments have found
a new type of matter...

SWEETNESS AND MIGHT

Awesome power of the glycome

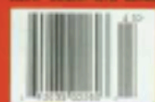
CHAD'S ANCIENT APE

Is this really the missing link?

LATEST NEWS

NASA's new vision emerges
Row over 'turning rivers around'
New scare links food to blindness

ISSN 0959-5294



nothing is known [4,5]. The discovery of such neutral systems as bound states would have far-reaching implications for many facets of nuclear physics. In the present paper, the production and detection of free neutron clusters is discussed.

The question as to whether neutral nuclei may exist has a long and checkered history that may be traced back to the early 1960s [5]. Forty years later, the only clear evidence in this respect is that the dineutron is particle unstable. Although 3n is the simplest multineutron candidate, the effects of pairing observed on the neutron drip line suggest that ${}^{4,6,8}n$ could exhibit bound states [6]. Concerning the tetraneutron, an upper limit on the binding energy of 3.1 MeV is provided by the particle stability of ${}^8\text{He}$, which does not decay into $\alpha + {}^4n$. Furthermore, if 4n was bound by more than 1 MeV, $\alpha + {}^4n$ would be the first particle threshold in ${}^8\text{He}$. As the breakup of ${}^8\text{He}$ is dominated by the ${}^6\text{He}$ channel [7], the tetraneutron, if bound, should be so by less than 1 MeV.

The majority of the calculations performed to date suggest that multineutron systems are unbound [4]. Interestingly, it was also found that subtle changes in the $N-N$ potentials that do not affect the phase shift analyses may generate bound neutron clusters [5]. In addition to the complexity of such *ab initio* calculations, which include the uncertainties in many-body forces, the $n-n$ interaction is the most poorly known $N-N$ interaction, as demonstrated by the controversy regarding the determination of the scattering length a_{nn} [8]. The

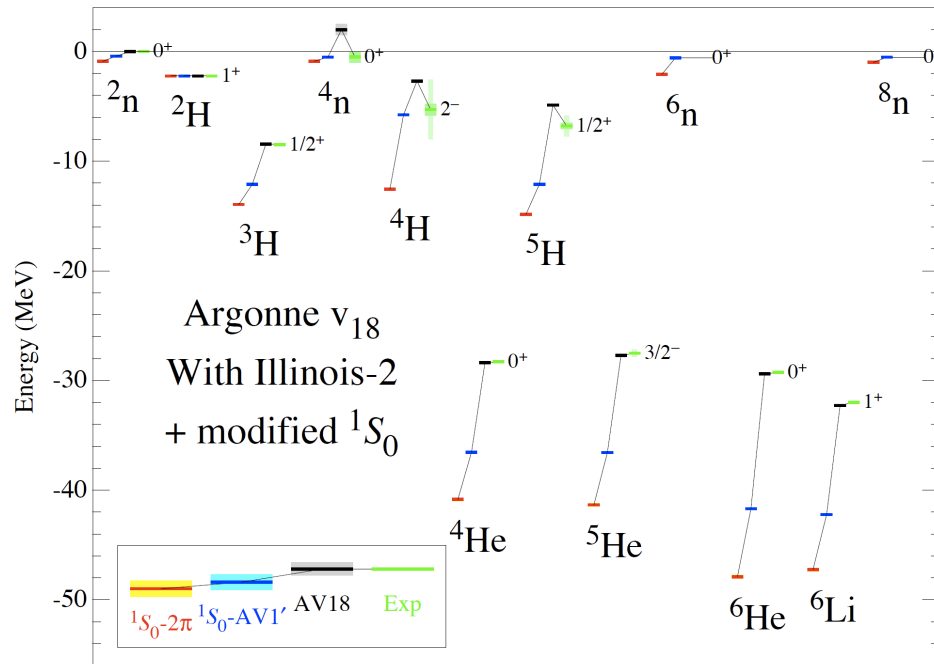
Can Modern Nuclear Hamiltonians Tolerate a Bound Tetra neutron?

Steven C. Pieper*

Physics Division, Argonne National Laboratory, Argonne, Illinois 60439, USA

(Received 18 February 2003; published 27 June 2003)

I show that it does not seem possible to change modern nuclear Hamiltonians to bind a tetra neutron without destroying many other successful predictions of those Hamiltonians. This means that, should a recent experimental claim of a bound tetra neutron be confirmed, our understanding of nuclear forces will have to be significantly changed. I also point out some errors in previous theoretical studies of this problem.



Theory does not support
the existence of a tetra neutron.

S. C. Pieper -- Fig. 3

FIG. 3: Energies of nuclei and neutron clusters computed with the AV18/IL2 Hamiltonian with modified NN potentials ($^1S_0-2\pi$ and $^1S_0-AV1'$) and with no modification (AV18), compared with experimental values for known nuclei.

Superheavy hydrogen isotopes.

**The most exotic system
ever found**

System with a $N/Z = 6$ can exist !
Gives important information on the
existence of a tetra neutron ($4N$).

Fitting to a Breit-Wigner distribution
the extracted resonance value is
0.57 MeV above the $3H+4N$ threshold
and with a width 0.09 MeV.

Need for theory

M. Caamano PRL 99, 062502 (2007)

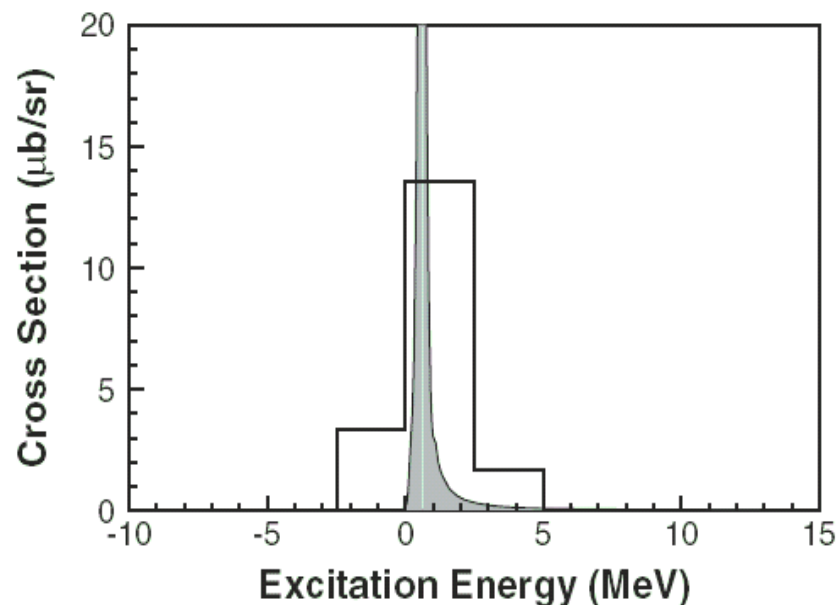
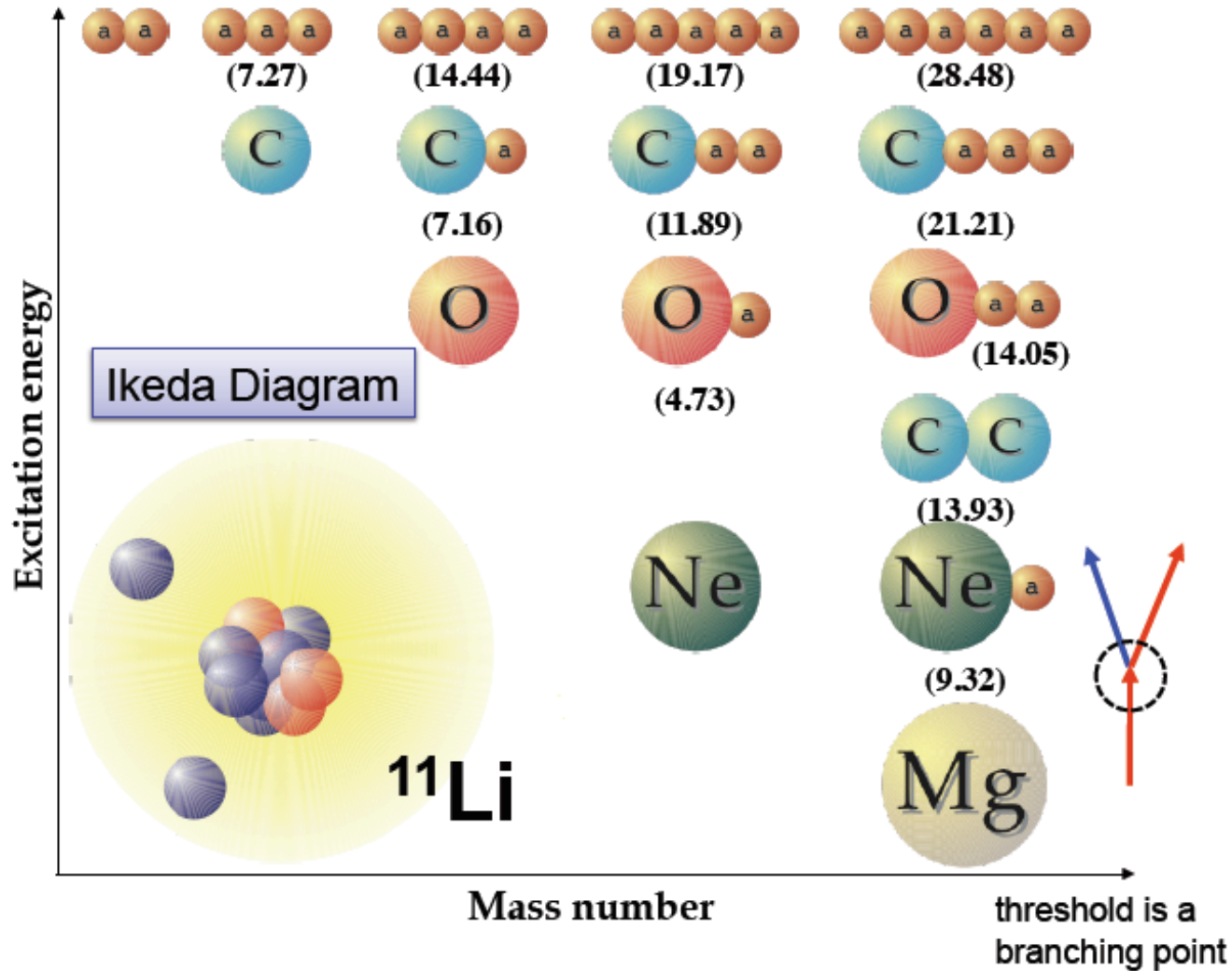
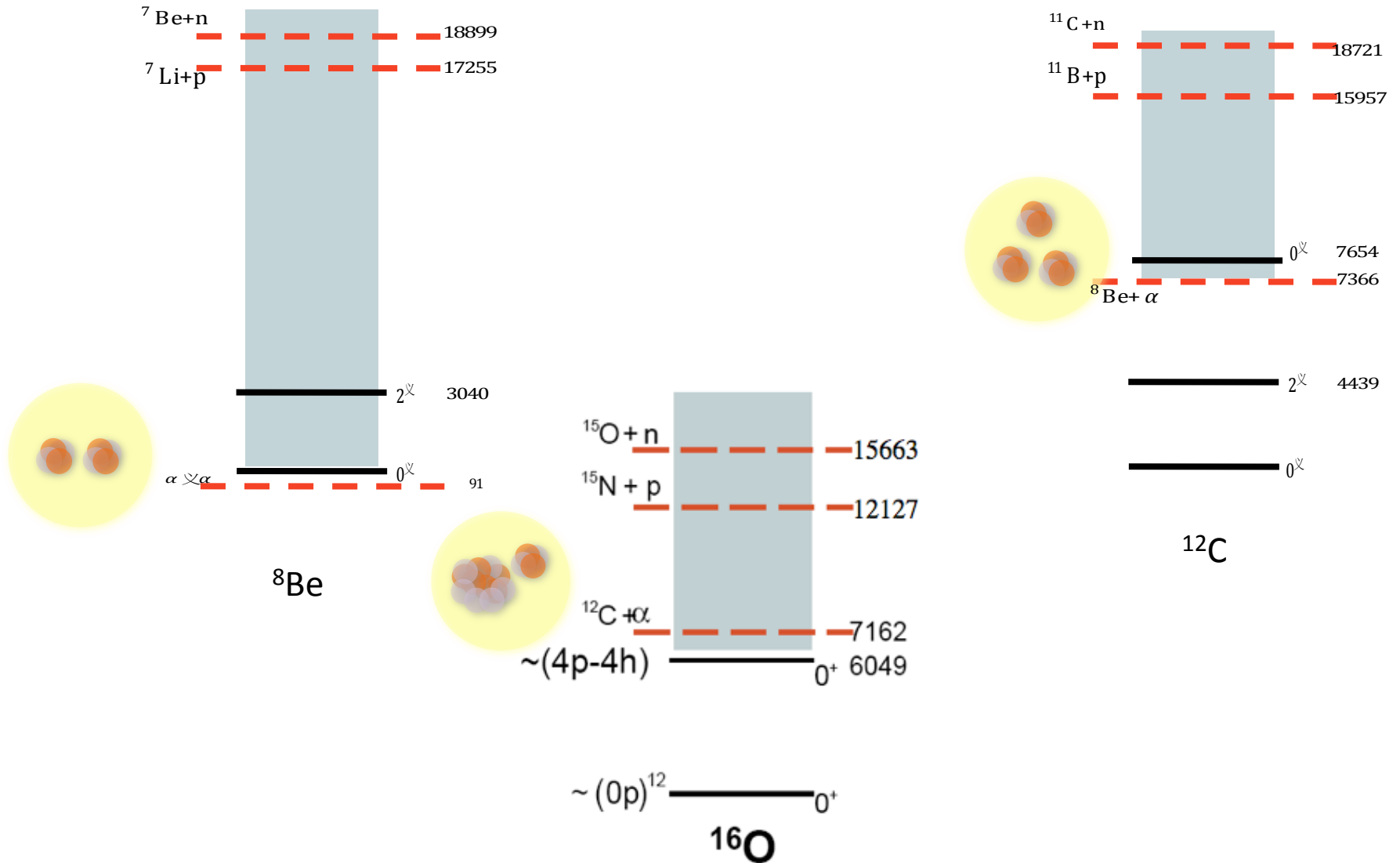


FIG. 4. Excitation energy distribution for the identified ${}^7\text{H}$ events. The solid function is the Breit-Wigner distribution resulting from the fit to the experimental events. The data are represented with the empty histogram merely as a guide to the eye, with a 2.5 MeV binning corresponding to the average estimated uncertainty.

Clustering in nuclei a near threshold phenomena



Cluster states near threshold.



Alpha Cluster Condensation in ^{12}C and ^{16}O

A. Tohsaki,¹ H. Horiuchi,² P. Schuck,³ and G. Röpke⁴

¹*Department of Fine Materials Engineering, Shinshu University, Ueda 386-8567, Japan*

²*Department of Physics, Kyoto University, Kyoto 606-8502, Japan*

³*Institut de Physique Nucléaire, F-91406 Orsay Cedex, France*

⁴*FB Physik, Universität Rostock, D-18051 Rostock, Germany*


(Received 29 June 2001; published 17 October 2001)

A new α -cluster wave function is proposed which is of the α -particle condensate type. Applications to ^{12}C and ^{16}O show that states of low density close to the 3 and 4 α -particle thresholds in both nuclei are possibly of this kind. It is conjectured that all self-conjugate $4n$ nuclei may show similar features.

DOI: 10.1103/PhysRevLett.87.192501

PACS numbers: 21.60.Gx, 03.75.Fi, 21.10.Gv, 27.20.+n

PRL **104**, 042701 (2010)

 Selected for a **Viewpoint** in *Physics*
PHYSICAL REVIEW LETTERS

week ending
29 JANUARY 2010



Novel Manifestation of α -Clustering Structures: New “ $\alpha + ^{208}\text{Pb}$ ” States in ^{212}Po Revealed by Their Enhanced $E1$ Decays

A. Astier,¹ P. Petkov,^{1,2} M.-G. Porquet,¹ D. S. Delion,^{3,4} and P. Schuck⁵

¹*CSNSM, IN2P3-CNRS and Université Paris-Sud, 91405 Orsay, France*

²*Institute for Nuclear Research and Nuclear Energy, Bulgarian Academy of Sciences, 1784 Sofia, Bulgaria*

³*Horia Hulubei National Institute of Physics and Nuclear Engineering 407 Atomistilor, 077125 Bucharest, Romania*

⁴*Academy of Romanian Scientists, 54 Splaiul Independentei, 050094 Bucharest, Romania*

⁵*IPN, IN2P3-CNRS and Université Paris-Sud, 91406 Orsay, France*

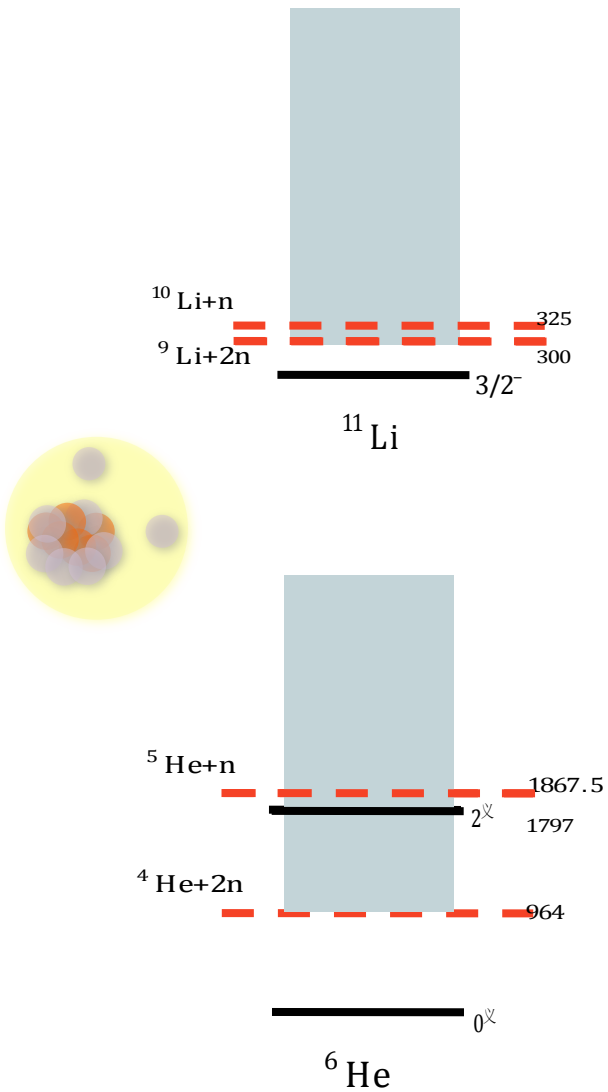
(Received 15 September 2009; published 25 January 2010)

Excited states in ^{212}Po were populated by α transfer using the $^{208}\text{Pb}(^{18}\text{O}, ^{14}\text{C})$ reaction, and their deexcitation γ rays were studied with the Euroball array. Several levels were found to decay by a unique $E1$ transition ($E_\gamma < 1$ MeV) populating the yrast state with the same spin value. Their lifetimes were measured by the Doppler-shift attenuation method. The values, found in the range 0.1–1.4 ps, lead to very enhanced transitions, $B(E1) = 2 \times 10^{-2}$ – 1×10^{-3} W.u. These results are discussed in terms of an α -cluster structure which gives rise to states with non-natural-parity values, provided that the composite system cannot rotate collectively, as expected in the “ $\alpha + ^{208}\text{Pb}$ ” case. Such states due to the oscillatory motion of the α -core distance are observed for the first time.

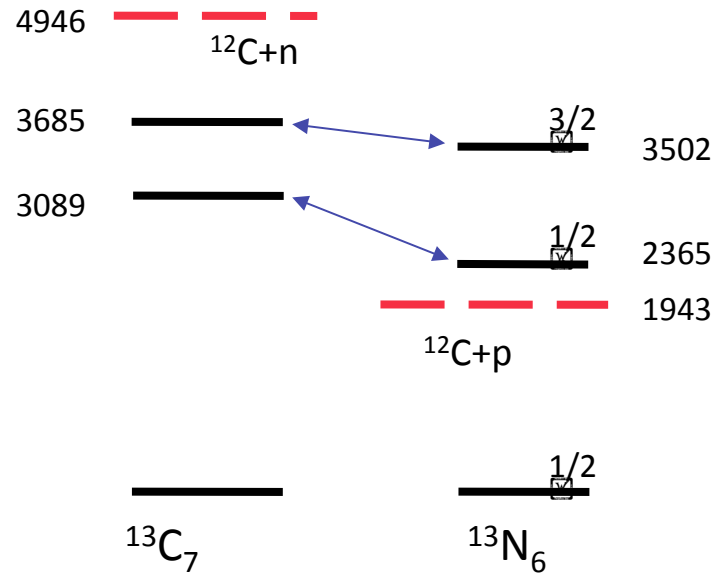
DOI: 10.1103/PhysRevLett.104.042701

PACS numbers: 25.70.Hi, 21.60.Gx, 23.20.-g, 27.80.+w

Halo structures



Thomas-Ehrmann effect



Spectra and matter distribution modified by the proximity of scattering continuum

Asymmetry dependence and spectroscopic factors

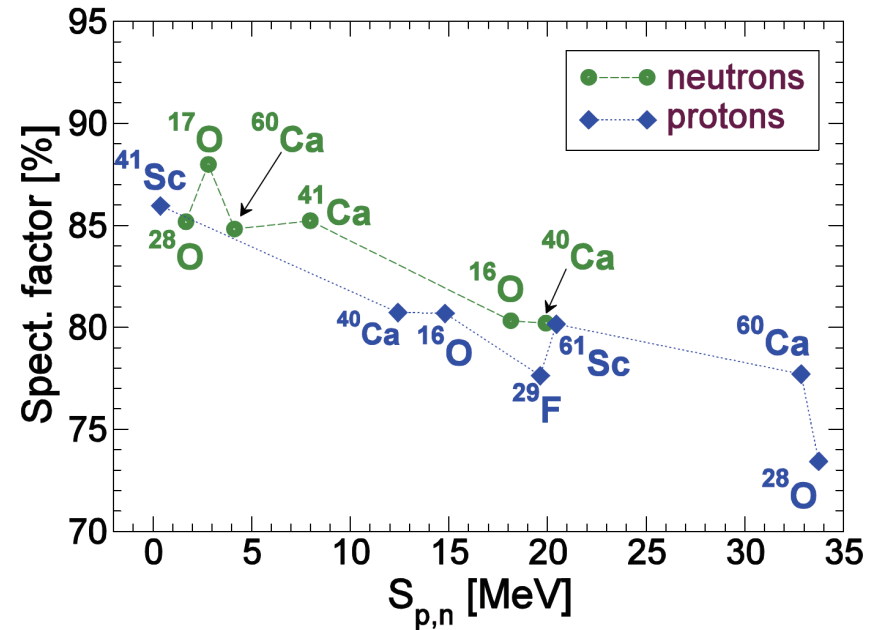
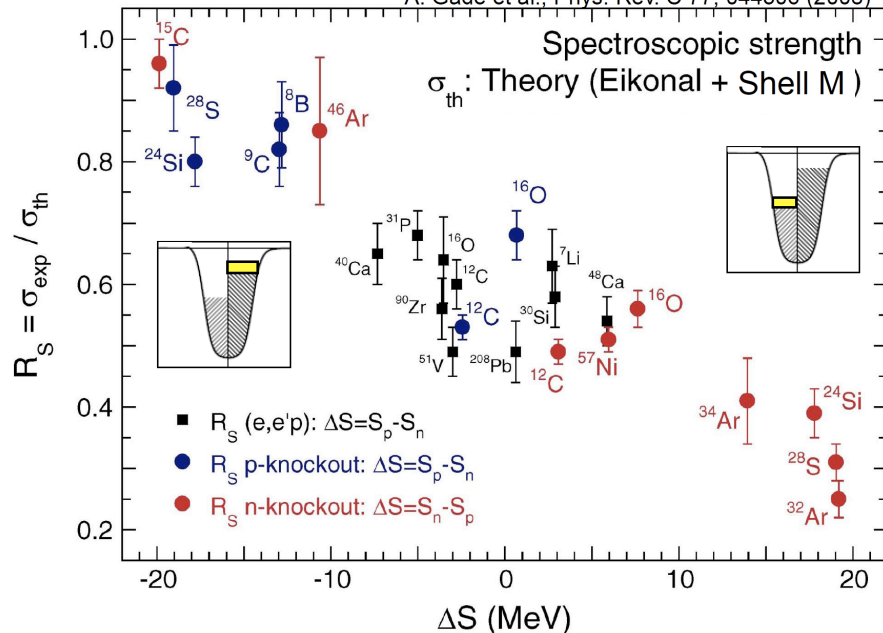
- Spectroscopic factors are not observables
- They are extracted from a cross section based on a specific structure and reaction model
- Structure and reaction models need to be consistent!

Theoretical cross section:

$$\sigma(j^\pi) = \left(\frac{A}{A-1} \right)^N C^2 S(j^\pi) \sigma_{sp}(j, S_N + E_x[j^\pi])$$

Reaction theory
Structure theory

A. Gade et al., Phys. Rev. C 77, 044306 (2008)



C. Barbieri, W.H. Dickhoff, Int. Jour. Mod. Phys. A24, 2060 (2009).

Self-consistent green's function method show rather weak asymmetry dependence for the spectroscopic factor.

Densities and radii from coupled-cluster theory

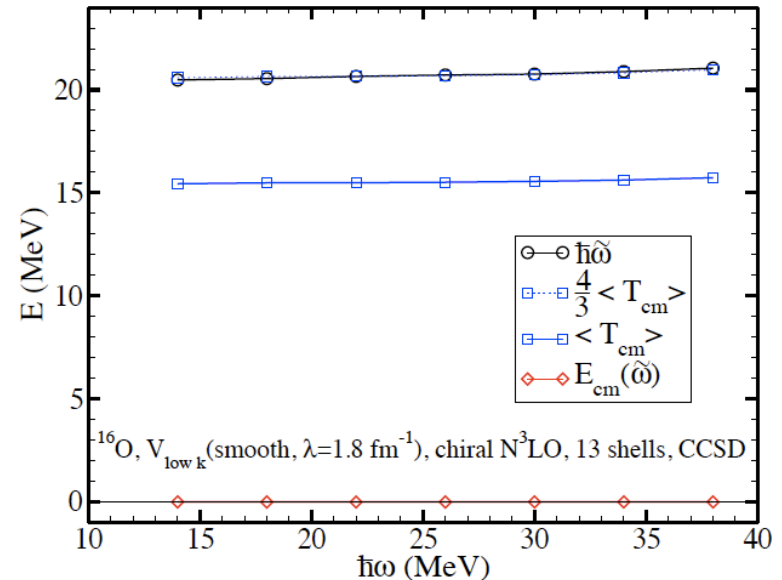
We solve for the right and left ground state of the similarity transformed Hamiltonian

$$e^{-T} H_N e^T |\phi_0\rangle = \overline{H}_N |\phi_0\rangle = E_{CC} |\phi_0\rangle \quad \langle \phi_0 | L_0 \overline{H}_N = E_{CC} \langle \phi_0 | L_0$$

The density matrix is computed within coupled-cluster method as:

$$\rho_{pq} = \langle \Psi_0 | a_p^\dagger a_q | \Psi_0 \rangle = \langle \phi_0 | L e^{-T} a_p^\dagger a_q e^T | \phi_0 \rangle = \langle \phi_0 | L a_p^\dagger a_q | \phi_0 \rangle$$

The coupled-cluster wave function factorizes to a good approximation into an intrinsic and center of mass part, $\Psi = \psi_{in} \Gamma$ where the center of mass part is a Gaussian with a fixed oscillator frequency independent of single-particle basis
 GH, T. Papenbrock and D. Dean et al, Phys. Rev. Lett. **103**, 062503 (2009)



We can obtain the intrinsic density by a deconvolution of the laboratory density

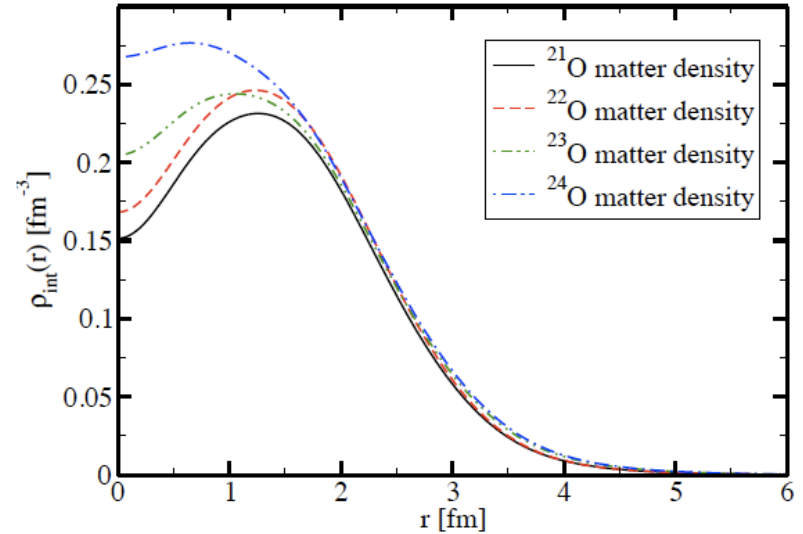
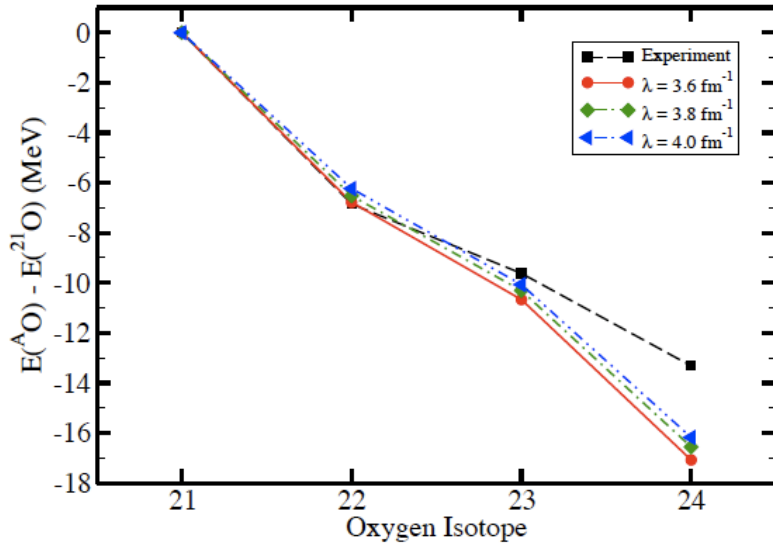
B. G. Giraud, Phys. Rev. C **77**, 014311 (2008)

$$A^{-1} \rho(r) = A^{-1} \int dR [\Gamma(R)]^2 \sigma \left[\frac{A}{A-1} (r-R) \right]$$

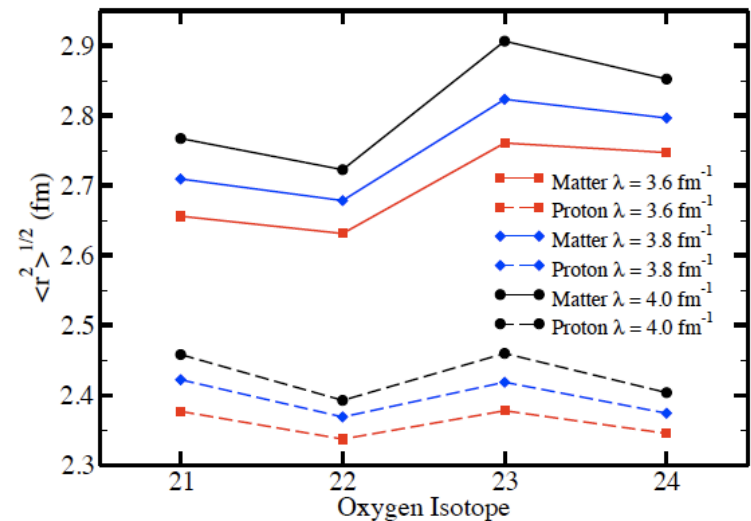
↑
↑
↑

Lab. density
Center of mass part
Intrinsic density

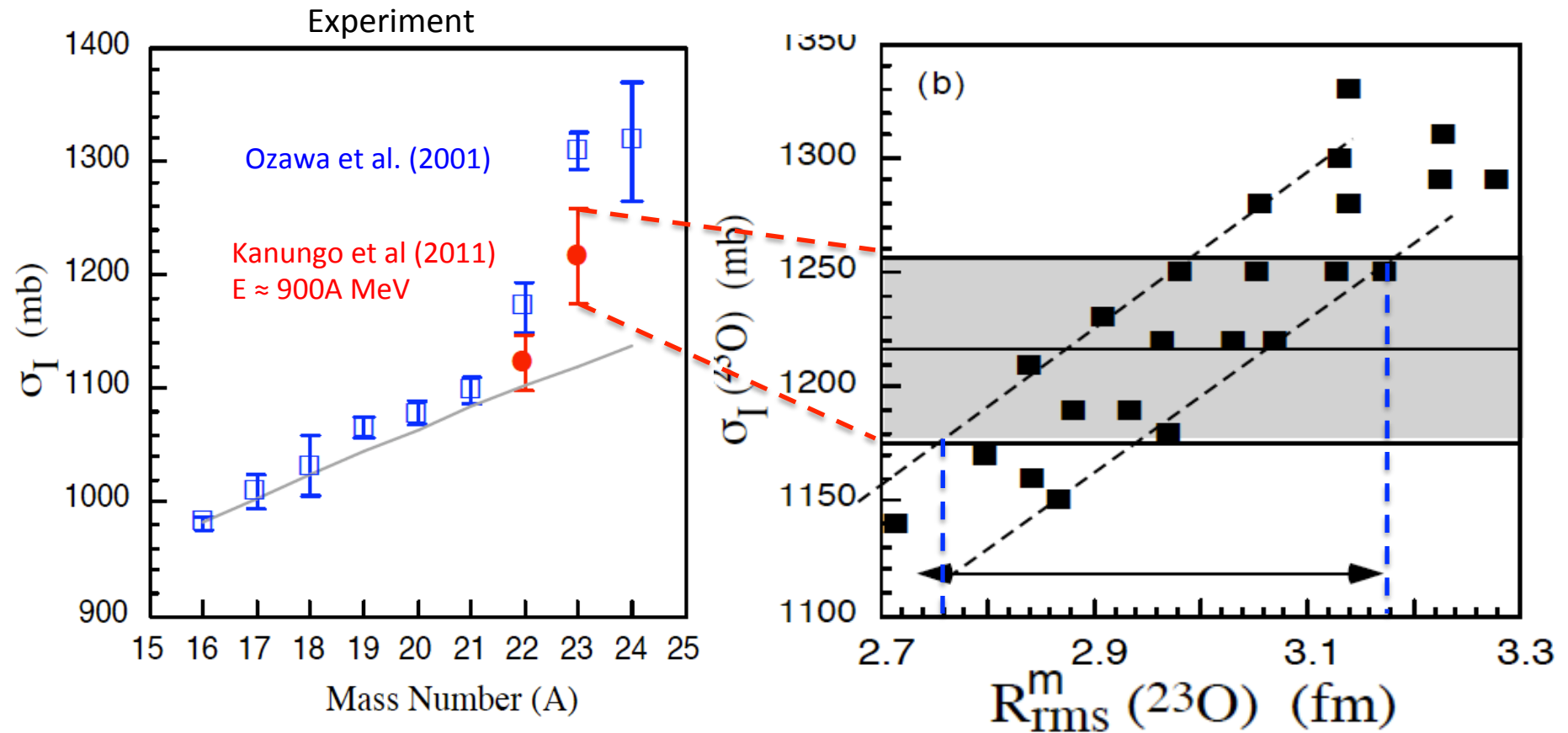
Densities and radii from coupled-cluster theory



1. Relative energies in $^{21-24}\text{O}$ depend weakly on the resolution scale
2. We clearly see shell structure appearing in the matter densities for $^{21-24}\text{O}$
3. Matter and charge radii depend on the resolution scale, however relative difference which is relevant for isotope shift measurements does not

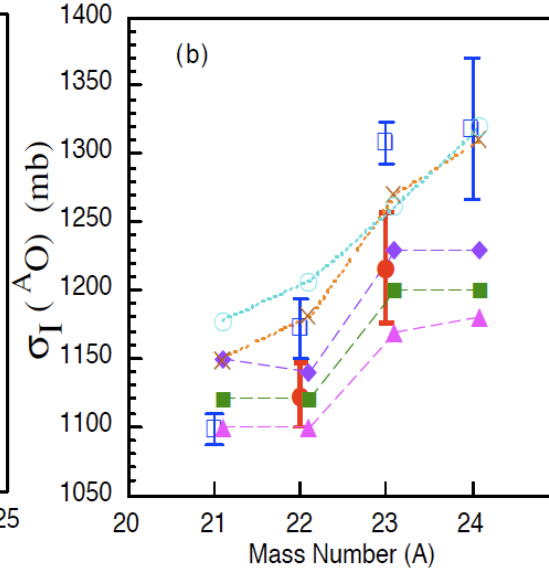
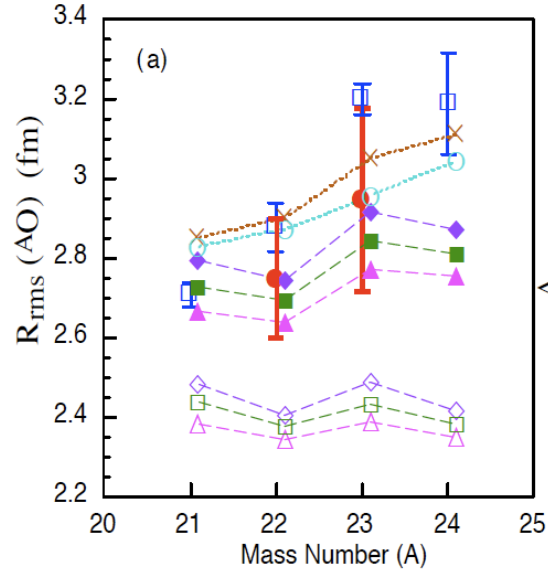


^{23}O interaction cross section (scattering off ^{12}C target @ GSI)



Experimental radii extracted from matter distribution within Glauber model.
 Main result of new measurement: ^{23}O follows systematics; interaction cross section consistent with separation energies.
 R. Kanungo *et al* Phys. Rev. C **84**, 061304 (2011)

Resolving the anomaly in the cross section of ^{23}O



The anomaly of ^{23}O

New measurements (R. Kanungo) of the ^{23}O cross section and coupled cluster calculations show that ^{23}O is not consistent with a one-neutron halo picture

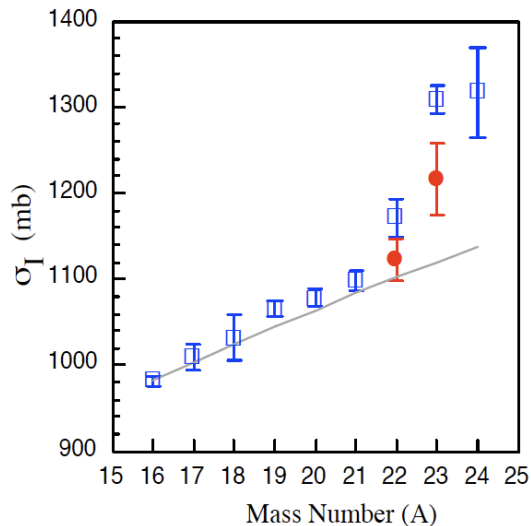


TABLE I: Measured interaction cross sections and the root mean square point matter radii ($R_{rms}^m(\text{ex.})$) for $^{22-23}\text{O}$.

Isotope	$\sigma_I(\Delta\sigma)$ (mb)	$\Delta\sigma(\text{Stat.})$ (mb)	$\Delta\sigma(\text{Syst.})$ (mb)	$R_{rms}^m(\text{ex.})$ (fm)
^{22}O	1123(24)	18.5	15.3	2.75 ± 0.15
^{23}O	1216(41)	33.1	24.7	2.95 ± 0.23

Oxygen isotopes from chiral interactions

- Inclusion of effective 3NF places dripline at ^{25}O .
- Overall the odd-even staggering in the neutron rich oxygen is well reproduced.
- We find ^{26}O to unbound with respect to ^{24}O by $\sim 100\text{keV}$, agreement with E. Lunderberg et al., *Phys. Rev. Lett.* **108** (2012) 142503
- We find ^{28}O to be unbound with a resonance width of $\sim 2\text{MeV}$

G. Hagen, M. Hjorth-Jensen, G. R. Jansen, R. Machleidt, T. Papenbrock, *Phys. Rev. Lett.* 108, 242501 (2012).

Chiral three-nucleon force at order N2LO. $k_f=1.05\text{fm}^{-1}$, $C_D = 0.2$, $C_E = 0.71$ (fitted to the binding energy of ^{16}O and ^{22}O).

